Lawrence Berkeley National Laboratory
Recent Work

Title

ALLOY DESIGN FOR FRACTURE TOUGHNESS

Permalink

https://escholarship.org/uc/item/3r62x9kh

Authors

Zackay, V.F.
Parker, E.R.

Publication Date

1974-06-01

ALLOY DESIGN FOR FRACTURE TOUGHNESS

V. F. Zackay and E. R. Parker

June 1974

DISCLAIMER

TABLE OF CONTENTS

ALLOY DESIGN FOR FRACTURE TOUGHNESS

by

V. F. Zackay and E. R. Parker

Center for the Design of Alloys, Inorganic Materials Research Division,

Lawrence Berkeley Laboratory and Department of Materials Science and

Engineering, College of Engineering; University of California,

Berkeley, California 94720

INTRODUCTION:

The most important mechanical property required of a structural

material is resistance to sudden or catastrophic fracture.   For this

reason, metals are usually the materials of choice where such failure

would result in loss of life or property.   The resistance of metals

to catastrophic failure is, however, not an intrinsic and fixed quantity.

On the contrary, it changes with the amount and type of stress, the

temperature, the strain rate, and environmental variables, i.e., macroscopic

factors, as well as with alloy composition and structure, i.e., microscopic

factors.   Consideration of only one set of these factors in either the

design of an engineering structure or, alternatively, in the design of an

alloy is inconsistent in principle and ineffective in practice.

This review describes some of the progress made in both the macro-

scopic and microscopic approaches to the problem of designing alloys with

superior fracture toughness.   Following a brief review of the striking

progress made in the past ten years in the macroscopic field of continuum

mechanics, the influence of the microscopic variables of composition,

defect structure, and microstructure are considered.   Illustrative examples

are taken from the authors' own research and from the literature.

DISCUSSION

I.   Historical Perspective

In a review of a field as active and varied as the fracture toughness

of metals, historical perspective can be helpful.   A simple but reliable

way of obtaining perspective is to peruse the published proceedings of the

national and international fracture conferences that have been held every

five to ten years since 1950.

A conference on the fatigue and fracture of metals was held at the

Massachusetts Institute of Technology in June, 1950.   The papers on

fracture toughness presented at this conference can be conveniently

grouped into the two categories mentioned previously, viz., macroscopic

and microscopic.   Several papers having the macroscopic viewpoint were

concerned with interpretating brittle failures in large structures such

as ships and planes.   These interpretations were made with the aid of

classical engineering stress analysis and were concerned with design

criteria such as the presence and configuration of notches, faulty

workmanship encountered in welding practices, and evaluations of the

quality of the steel by macroscopic observations of fracture surfaces.

In other papers with the macroscopic viewpoint, the tendency for brittle

fracture in steel, measured by either the Charpy, notched tensile or slow

bend test, was discussed in terms of the shift of the ductile-brittle

transition temperature.   The influence of test variables such as temperature,

strain rate, notch acuity, and composition was recognized but was difficult

to reconcile into a unified theory.   The variation of transition temperature

with type of specimen and nature of test obviously posed great difficulties

in analysis to the conference attendees. It is of interest to note that one paper in the microscopic category, given by Orowan, is now regarded as a historical milestone in the development of a quantitative theory of fracture toughness. Orowan suggested that the surface energy term, γ, in the Griffith theory of fracture as applied to metals, be substituted by a term, E_p, which symbolized the energy absorbed by microscopic plastic flow in front of the moving crack. Lastly, the conferees were well aware of the importance of the role played by microstructure in temper embrittlement and in fatigue failures, but their knowledge of defect structure and microstructure was limited by the low resolution of the available instrumentation for the characterization and identification of structure.

The international conference on fracture held in Swampscott, Massachusetts in April, 1959, must be considered a major event in the progress toward a comprehensive treatment of the fracture of solids. Although less than a decade had passed since the 1950 conference, tremendous advances had been made in the understanding of the atomistic and microstructural features of fracture in metallic, ceramic and polymeric materials. So much significant progress was reported at this conference that it is difficult to select the most important advance. It was, however, abundantly clear that one outstanding achievement was the application of dislocation theory to both the theoretical and experimental aspects of fracture. Further, the importance of microstructural features such as slip bands, twins, grain boundaries, and brittle phases was qualitatively delineated in metals and in some ceramics for fracture under static, dynamic, and cyclic types of loading at both room and elevated temperatures. One prominent feature of the conference was the reported use of new high

resolution tools such as the electron microscope to characterize the interior structure and the fracture surface morphology (by replication techniques).

The sessions on cleavage fracture, ductile fracture and fatigue, and elevated temperature fracture were summarized by Barrett, Honeycombe, and Grant, respectively. They restated some of the pivotal unanswered questions raised during the conference. Conferees agreed that the Griffith equation was satisfactory as a first approximation (in its modified form) but questioned whether it could be made more quantitative or that it would ever be capable of predicting the effect of variables such as temperature and strain rate on the fracture of solids. Another conference question related to the disproportionate emphasis on the fracture behavior of relatively simple materials, i.e., single and bicrystals of pure metals. Relatively little understanding had been gained with respect to the fracture of the more complex materials of engineering structures. Last, and perhaps most significant, relatively little had been accomplished to reconcile the atomic and microscopic views of fracture with the macroscopic ones of mathematical plasticity --- an essential linkage if new and superior engineering materials were to be developed from the first principles of materials science. It is interesting --- and satisfying --- that all of these questions were partially or completely answered within the next decade.

In the ensuing fifteen years, there were many national and inter-national conferences on the subject of fracture, as well as several new journals and many new books. The topic of fracture, always intensely interesting to scientists and engineers for obvious reasons, has become

one of the most popular areas of research in physical metallurgy. Why
is this so? What has happened to bring about this explosion of interest?
Clues to the answers to these questions are found in the questions
raised at Swampscott. As mentioned previously, the conferees at
Swampscott had difficulty, in spite of their successes, in reconciling
the atomistic and microstructural views of fracture as enunciated primarily
by materials scientists, with those of macroscopic mathematical plasticity
as promulgated largely by engineers. This difficulty was also reflected
in the type of materials that were being studied, viz., most of the
experimental effort was on single crystals and/or high purity metals
instead of the complex alloys used in engineering structures.

A series of papers by Irwin and his colleagues in the late 1950s
and early 1960s dramatically solved these problems. This pioneering
work introduced concepts which have led to significant progress in the
unification of the microscopic and macroscopic views of fracture.
Perhaps most significant of all, the practical application of these
concepts has already proven effective in reducing the possibility of
catastrophic fracture in engineering structures.

The original data of Irwin and his colleagues were expressed in
terms of the critical value of the strain (or potential) energy release
rate G_C, at which unstable crack propagation occurred. Irwin's basic
approach was, therefore, analogous to Griffith's, viz., a thermodynamic
one. Irwin's approach provided a convenient parameter to include all
supplementary energy-dissipating terms, such as plastic flow, which
could in turn produce heat or sound, in addition to the work required
to fracture the lattice. The constancy of G_C, and hence its use as a

measure of the resistance of a material to fracture depends critically on experimental testing conditions, but for situations where plastic flow preceding crack extension is small and localized within a small area, the critical value can always be related to the failure stress using linear elastic methods. Irwin's parameter, G_C, became known as "fracture toughness," although this term is now generally reserved for the associated value of critical stress intensity, K_C.

The disadvantage of using the critical strain energy release rate, G_C, is that fracture is considered, although indirectly, in terms of a complex energy concept. This difficulty is removed if fracture is considered in terms of the elastic stress components adjacent to the crack tip. Westergard showed that the stress σ_y in the direction normal to the plane of the crack, and at a point (on the crack plane) distant "r" from the crack tip, reduced to the following expression:

$$\sigma_y = K\sqrt{2\pi r}$$

where K is the stress intensity factor. For elastic loading the strain energy is uniquely defined by the stress distribution. Thus, a simple relationship exists between the stress intensity factor K and the strain energy release rate G. For plane stress, $K_C^2 = G_C E$ while for plane strain, $K_{IC}^2 = \dfrac{G_{IC} E}{1 - \nu^2}$ where ν is Poissons ratio and E is Young's modulus of elasticity.

The only section of fracture mechanics which has so far been rigorously formulated is that of linear elastic fracture mechanics although much progress is being made in non-linear concepts such as the "J-integral" approach. Thus, at present, fracture mechanics can be used only for

elastic brittle materials or materials which approach this limit.
Examples are high strength aluminum alloys, glass, high strength steel
(the fracture characteristics of these materials are relatively
insensitive to temperature and strain rate) and the propagation, but not
the initiation, of a crack in low strength steel under cyclic loading.
Thus, designing against brittle fracture requires two approaches, one
for strain rate- and temperature-sensitive materials --- the transition
temperature approach --- and the other for strain rate- and temperature-
insensitive materials --- the fracture mechanics approach.

Both the above-mentioned approaches have been discussed in detail
in the recent literature. Some representative reviews are given below.
Tetelman and McEvily (1967), in their book entitled, "Fracture of
Structural Materials," comprehensively discuss both the transition
temperature and the fracture mechanics approaches. The relative roles
of composition and microstructure are treated in both these approaches.
Knott (1973), in a recent monograph entitled, "Fundamentals of Fracture
Mechanics," concisely and rigorously develops the historical evolution
of fracture mechanics in a manner useful to both the designer and the
physical metallurgist.

In a provocative study, Averbach (1968) derives quantitative relation-
ships between the macroscopic and the microscopic variables of fracture
of simple solids. Pellini and his coworkers have been pioneers in the
transition temperature aspect of fracture. Recent papers by Pellini (1968),
Puzak and Lange (1969), and Loss and Pellini (1969) are representative
of their work. For a detailed and comprehensive review of the whole

field of fracture the series of volumes edited by Liebowitz (1968) is

invaluable.   Lastly, the Proceedings of the Second Tewksbury Symposium,

edited by Osborn et al. (1969) is a thoughtful review of the progress

made in applying what is currently known about fracture to the design

of useful engineering structures.   Much of the foregoing discussion

was based on the review papers of this symposium and on the discussion

of the evolution of modern fracture mechanics by Knott (1973).

I I.   Designing for Toughness

In the ensuing discussion, examples of both the transition temperature

and the fracture mechanics approaches to the design against brittle

fracture are presented.   The relationships between the macroscopic and

microscopic viewpoints are stressed.   In each case, the objective was

to achieve, through compositional and microstructural control, improved

combinations of strength, ductility and toughness.

A.   The Transition Temperature Approach

Metals or alloys with the bcc structure can fail either by shear

or by cleavage.   It is now well established that the propensity of bcc

metals to fail by cleavage is influenced by a host of compositional and

structural variables.   The temperature of transition from a high energy

shear fracture to a low-energy cleavage fracture, for a given type of

test, is a convenient measure of the influence of these variables.   Some

of the compositional and structural variables known to decrease the

transition temperature in bcc iron-base alloys are: (1) the lowest

possible level of interstitials in solid solution (interstitials raise

the critical resolved shear stress of bcc metals to the cleavage stress

as the temperature is lowered),   (2) the maximum amounts of either nickel

or manganese in solid solution commensurate with other metallurgical

considerations, and (3) the finest possible grain size. This listing

of desirable features is, of course, not complete and is intended only

as a guide for the selection of an alloy system for study. The system

Fe-Ni-Ti appears to be particularly appropriate for such a study. The

titanium and nickel contents in these alloys can be varied to meet

requirements (1) and (2) above. Fine grain sizes can be obtained by

thermal or thermal-mechanical means. In the investigation summarized

in the following discussion the nickel content was varied from 8 to 16%

while the titanium content was kept constant at 0.5%. Details of this

and related work are given in the papers by Horwood (1972), Sasaki (1973),

Zackay (1973), Jin et al. (1973 a,b,c), Yokota et al. (1974 a,b), and

Sasaki et al. (1974).

The change in the impact toughness at -196°C of specimens of an

Fe-12% Ni-0.5%Ti alloys as a function of thermal and thermal-mechanical

history is summarized in Fig. 1. All specimens were given a 900°C

solution treatment and then reheated to the temperatures indicated prior

to testing at -196°C. The range of reheat temperatures included the

lower and upper limits of temperature of the two phase ($\alpha + \gamma$) region

(shown by the horizontal broken lines in the figure) as well as the

lower part of the single phase (γ) region. The Charpy impact energies

showed a gradual increase with reheat temperature in the upper limit

of the two phase ($\alpha + \gamma$) region. Abrupt increases in impact energy were

observed when the reheat temperatures were inside of a one hundred degree

range which was above the lower limit of the single phase (γ) region, as

shown by curve A. Reheat temperatures above this range, however, resulted in a sharp decline in impact toughness, as shown in the figure. All specimens exhibiting the peak Charpy values were characterized by micro-structures having a fine grain size, while those with low values were coarse grained. Electron microscope examination by replication techniques suggested that new grains formed at prior austenitic and martensite lath colony boundaries via dissolution of the two phase ($\alpha + \gamma$) duplex structure which had formed on heating.

Substantiation of this apparent grain refining mechanism was obtained by systematically varying the thermal history of specimens. Specimens were first heated to 650°C prior to raising the reheat temperature to between 750-800°C. This initial low temperature treatment resulted in broadening the reheating temperature vs. Charpy energy curve as shown in Fig. 1, curve B. The microstructures of specimens within the peak region delineated by curve B were, as expected, single phase and fine grained. A similar improvement in toughness and associated microstructures was produced by a process essentially equivalent to that described above, viz., by slowly heating the specimens through the two phase ($\alpha + \gamma$) region on the way up to the higher temperatures. Cold working prior to reheating produced an even finer grain size at the reheating temperatures investigated. The Charpy energy as a function of reheating temperature for the cold worked specimens is shown in Fig. 1, curve C.

The relationship between the refined prior austenite grain size and the resulting impact toughness is given in Fig. 2, in which the impact energy at -196°C is plotted vs. the grain size for the several grain refining treatments described above. The results showed that regardless

of the grain refining method used, there was a sharp drop in impact energy
above a critical grain size of about 15 microns. Similar relationships
existed for all the alloys investigated. For the 8% Ni alloy, the
critical grain size was about 5 microns, and for the 16% Ni alloy, about
30 microns.

Studies of the type described above established useful relationships
between nickel content, grain size and impact toughness for a family
of nickel-containing and titanium-stabilized alloys. Practical implementation
of these studies could eventually result in the design of cryogenic
steels with desirable combinations of strength, ductility, and toughness.

B. The Fracture Mechanics Approach

1. Metastable Austenitic Steels

The mechanical properties of steels with a metastable austenitic
matrix are known to be highly dependent on the composition, the temperature
of testing, the state of stress, the prior history of processing, and
the strain rate (Bhandarkar et al., 1972). In some alloy systems a
phase transformation may be initiated by elastic or plastic deformation.
Some commercial stainless steels (AISI Type 300 series) undergo an
austenite to martensite phase transformation when deformed. However,
these commercially available steels have relatively low yield strengths.
In a recent development, deformation induced phase transformations were
utilized to create a new class of ultra-high strength metastable austenitic
steels, known as TRIP steels (Zackay et al., 1967). (The word TRIP is
an acronym of transformation induced plasticity.) The alloy content of
TRIP steels is adjusted so that the face centered cubic phase is thermally
stable at room temperature. When these alloys are deformed, they transform

to the body centered martensitic phase, and fracture is attended by a
considerable amount of plastic deformation even at high strength levels.
Both the plastic deformation and the transformation enhance energy absorption
at the tip of a moving crack and result in a higher critical energy release
rate (G_{IC}) for crack propagation. This suggests that a fracture mechanics
approach can be fruitful in designing high strength TRIP steels with high
toughness.

The fraction of the volume that transforms for each unit of strain
depends upon austenite stability, which in turn is determined by the
composition, the prior history, the test temperature, and the test strain
rate. The uniform elongation, rate of work hardening, yield strength,
ultimate tensile strength, and fracture toughness are all strongly
influenced by the stability of the austenite, as is shown in detail in
a later section.

In a recent study, Bhandarkar et al. (1972) determined the influences
of composition, processing conditions, and test temperature on the
stability of austenite. Parts of the following discussion are based
upon the results of their study. The chemical compositions of several
of the steels involved are given in Table I. All the alloys listed
were deformed 70% at a temperature of 450°C, unless otherwise designated.
The primary purpose of such prior deformation of the austenite in TRIP
steels is to raise the yield strength, often to 200,000 psi or more.

It is possible to obtain experimentally an austenite stability
index for TRIP steels. With this index, predictions can be made of
the effect of composition and processing conditions on mechanical

properties. Gerberich et al. (1970) have suggested that the volume fraction of martensite, V_α, produced during a tensile test varies as

$$V_\alpha = m\epsilon^{\frac{1}{2}}$$

where m is a constant for a given set of test conditions and ϵ is the conventional strain. The transformation coefficient, m, was found to be a useful index of austenite stability, with higher values of m indicating lower degrees of stability. The value of m is readily obtained by plotting V_α vs. $\epsilon^{\frac{1}{2}}$ and fitting the best straight line to the plot. Typical experimental data for steel CN8Cr are shown in Fig. 3 for a test temperature of -78°C. In TRIP steels the coefficient m can be varied from zero (completely stable) to about 3.5 (highly unstable). The value of m is zero when the test temperature is at or above the M_d temperature --- the temperature above which plastic strain will not induce a transformation. Another phase transformation temperature of importance in these steels is the M_s, which is the temperature at which martensite starts to form in an unstressed steel during cooling. The M_s is always below the M_d. TRIP steels are designed to be used at service temperatures between the M_s and M_d. In this temperature range, the austenite is thermally stable with respect to the service temperature but unstable with respect to strain. At temperatures well below the M_d and close to the M_s, the steel becomes so unstable that even an elastic deformation can induce a transformation (Scheil, 1932; Kulin et al., 1952; Angel, 1954; Fahr, 1969 and 1971; and Bhandarkar et al., 1972).

Bhandarkar et al. (1972) demonstrated the relationships between stability and mechanical properties for steels with stabilities varied by changes in test temperature (22° to -196°C), composition, (8, 12, 16, and 21% of Ni) and the prior deformation temperature (25° to 450°C). Examples of their results are shown in Figs. 4 and 5.

The engineering stress-strain curves at 22°C and -78°C are shown in Fig. 4 for the CN8Cr steel (composition given in Table I) deformed 70% at 450°C. The m values are also shown in the figure. The stress-strain curve obtained at 22°C exhibited a well-defined Lüders strain of about 6%, a low strain hardening rate, and an elongation of 20%; the m value was 1.85. The relatively low rate of strain hardening was a consequence of the comparatively low rate of martensite formation with strain. At a test temperature of -78°C, the stress-strain curve was quite different. The yield strength was lower by about 60,000 psi than that at 22°C, the Lüders strain was smaller and less well defined, the rate of strain hardening was much higher, and the elongation was about one-half of the room temperature value. These features are a consequence of the change in the stability produced by the temperature change (as reflected by the m value). Of particular interest are the low yield strength and the high rate of strain hardening. These features are characteristic of an alloy undergoing a stress induced phase transformation. At a strain of only 0.02, about half the austenite had already transformed to martensite in the -78°C test, as shown in Fig. 3. In the specimen tested at 22°C, less than 10% of the austenite had transformed at the same strain.

The stability can also be altered by changing the chemical composition or the prior deformation temperature. The stress-strain curves for three steels of different nickel contents, deformed 70% at 450°C and tested at -78°C, are shown in Fig. 5 (Bhandarkar et al., 1972). The striking difference between the curves is worthy of note. As Bressanelli and Moskowitz (1966), Gerberich et al. (1970), and Tamura et al. (1970) have observed, maximum elongation results when martensite is produced at an optimum rate with strain. Too little martensite forming per unit of strain results in early necking and too much causes premature failure. The relatively low m value for steel CN12Cr (estimated to be between 1.0 and 1.5) indicates that the criterion of an optimum m value for a large elongation has been met.

Changes in stability markedly influence the shape of stress-strain curves because Lüders strain, strain hardening rate, and elongation to fracture are affected by stability changes. In Fig. 6 are shown plots relating the stability coefficient, m, with elongation to fracture (Fig. 6(a)) and Lüders strain (Fig. 6(b)) for a large group of alloys of widely varying composition, processing histories, and testing temperatures (Gerberich et al., 1970).

Several investigators have suggested that a stress or strain induced phase transformation might enhance the absorption of energy and thereby increase fracture toughness (Gerberich et al., 1968, 1969, and 1971; Antolovich, 1968; Gerberich and Birat, 1971; and Antolovich and Singh, 1971). The fracture toughness of TRIP steels has been studied from both the theoretical and experimental viewpoints. It is clear from these studies that the toughness is dependent upon the stability, the chemical composition

of the strain induced martensite, and the strain rate. Gerberich et al. (1971) have shown that, as a first approximation, the fracture toughness K_C, is proportional to $m^{\frac{1}{2}}$. Room temperature plane stress fracture toughness values of almost 500,000 psi-in$^{\frac{1}{2}}$ were reported for highly unstable (m = 2) steels having yield strengths of 200,000 psi or higher; a summary of the data is shown in Fig. 7. The fracture toughness is decreased with increasing amounts of carbon plus nitrogen in an alloy. The effect of carbon and nitrogen contents on the apparent K_{IC} value at -196°C is shown in Fig. 8. Fractographic analysis showed that the martensite in the higher carbon steels (over 0.27%) had a tendency to fail by cleavage rather than by shear. The variation with carbon content of apparent K_{IC} values at -196°C reflects this change of fracture mode.

Gerberich et al. (1969) and Antolovich and Singh (1971) have derived analytical expressions which include the contribution of the phase transformation to the observed fracture toughness of TRIP steels. Both groups of investigators have concluded from theoretical and experimental evidence that the phase transformation is a major source of their fracture toughness. Antolovich and Singh (1971) experimentally determined this contribution to be between two-thirds and three-fourths of the measured crack extension force, G_{IC}. However, no attempt has yet been made (to the authors' knowledge) to estimate the change in stress state existing near the tip of a crack in a steel undergoing a stress- or strain-induced transformation. This is a very important factor. When austenite transforms to martensite, there is a volume

increase of about 3%. This corresponds to a linear increase of 1% in each of three perpendicular directions. This volumetric expansion effectively cancels a large part of the triaxial stress that exists near the root of a sharp crack or notch. The reduction in the triaxial component of stress has a marked effect on the behavior of thick specimens, where triaxiality is a major contributor to brittle behavior. As a consequence, TRIP steels exhibit an unusual variation in fracture toughness with specimen thickness. The fracture toughness of virtually all high strength alloys decreases sharply with increasing thickness. This does not appear to be the case with TRIP steels. As shown in Fig. 9, the critical stress intensity factors (K) at room temperature of both the low alloy quenched and tempered steel and the precipitation hardening stainless steel decrease with thickness more severely than those of the TRIP steel (Gerberich et al., 1971).

It has been shown both analytically and experimentally that the rate of production of strain induced martensite decreases with increasing crack velocity because of adiabatic heating (Dokko, 1969, and Gerberich et al., 1971). The consequence is a decrease in the fracture toughness.

The powerful beneficial effect of the transformation of metastable austenite on the fracture toughness of steels apparently persists even when the metastable retained austenite is a minor constituent in a bcc iron matrix. This aspect of alloy design is discussed in the next section.

2. Quenched and Tempered Steels

Ultra-high strength steels are relatively brittle, and their mechanical properties are not sensitive to small changes in temperature and strain rate. Application of the fracture mechanics method of

analysis to alloy design is therefore natural (Knott, 1973). It should

be recalled that the first rests on Irwin's pioneering concepts in fracture

mechanics were made on this class of steels.

A voluminous literature now exists on both the macroscopic and

microscopic aspects of fracture of ultra-high strength steels. No

attempt is made in this report to review the literature in its entirety;

rather, a few typical examples are used to illustrate progress made

in the design of experimental steels with combinations of strength and

toughness superior to those commercially available.

Several years ago, an extensive program was undertaken at the

authors' laboratory on the fracture toughness of high strength steels.

One principal objective in this study was to identify and characterize

those elements of defect structure and microstructure that influenced the

plane strain fracture toughness. It was surmised that some elements of

structure would enhance, while others would degrade, the fracture toughness.

In the planning phases of this program it was assumed that weak or brittle

microconstituents would degrade fracture toughness while others might

prove beneficial. For example, the lamellar or plate-like forms of

ferrite and cementite which occur in pearlitic and upper bainitic micro-

structures were considered to be detrimental. Similarly, the presence

of both non-metallic inclusions and undissolved brittle carbides was

thought to be undesirable. Also, evidence suggested that twinned

martensite plates, as opposed to untwinned plates or laths, were detrimental.

On the beneficial side, there was speculation and some evidence that

retained austenite might, under certain circumstances, improve the

fracture toughness of high strength steels. Accordingly, a series of

heat treatments was devised for both commercial and laboratory-type steels

with the objective of minimizing the deleterious compositional and structural features while maximizing the beneficial ones.

A critical phase in the heat treatment of any steel is the austenitizing step. During austenitization many compositional and structural changes occur and profoundly influence the final microstructure and its associated mechanical properties. For example, low austenitizing temperatures favor a small austenite grain size but may leave a larger fraction of brittle undissolved carbides. Conversely, high austenitizing temperatures lead to dissolution of a greater proportion of such carbides but cause a concomitant increase in austenite grain size. The complex and often unpredictable net effect of using a particular austenitizing temperature led, therefore, to a detailed study of its influence on the strength and toughness of a number of commercial and laboratory-type steels.

a. Austenitizing Temperature and Undissolved Alloy Carbides

As previously suggested, the presence of large undissolved particles of alloy carbides is likely to result in a deterioration of fracture toughness. The volume fraction and size of undissolved carbides left in the austenitic matrix prior to quenching, for a given composition, varies inversely with the austenitizing temperature. In an effort to evaluate relationships between austenitizing temperature, volume fraction of undissolved carbides, fracture toughness, and strength, several laboratory-type secondary hardening steels were studied. Their compositions are shown in Table II.

The effect of varying the austenitizing temperature on the room temperature yield strength, ultimate strength and the fracture toughness of as-quenched 0.30C-5Mo and 0.41C-5Mo steels is shown in Fig. 10 (T. Tom, 1973). In general, both strength and fracture toughness increased

with increase in the austenitizing temperature. The increase in fracture
toughness with austenitizing temperature for the lower carbon steel was
particularly striking. Metallographic examination of these high
molybdenum steels indicated that extensive solution of alloy carbides
occurred above a critical austenitizing temperature. The fracture
toughness was observed to increase markedly in the same temperature range.
Associated with the increased solution of carbides and the improved fracture
toughness was, as expected, a pronounced increase in grain size. Similar
experiments were performed with another set of lower alloy steels in which
complete dissolution of carbides could be effected at austenitizing
temperatures as low as 870°C. In this instance the fracture toughness
of either steel was relatively independent of the austenitizing temperature
(or grain size) as shown in Fig. 11.

Transmission electron microscopic studies using carbon replicas
indicated that an austenitizing temperature of 870°C left undissolved
carbides of approximately 0.05 microns in diameter for a 0.32C-2Mo steel,
and of 1-3 microns for the 0.30C-5Mo steel, as shown in Figures 12 and 13,
respectively. The deleterious effects of the larger carbides was
suggested by the values of the ratio of plane strain fracture toughness
to yield strength for the two steels in the as-quenched condition.
These were 0.42 for the 0.32C-2Mo steel and 0.27 for the 0.30C-5Mo steel.
Furthermore, the ratios were equal for the 0.32C-2Mo steel austenitized at
870°C and the 0.30C-5Mo steel austenitized at 1200°C. These results
strongly indicated that the presence of hard, brittle undissolved particles
above a certain critical size could lead to a significant degradation of
the fracture toughness of alloy steels. The results also suggested that

the fracture toughness was insensitive to large variations in prior

austenite grain size for those alloy steels whose matrix was free of

undissolved carbides of sizes above a critical value. Additional

information on these steels is found in the investigations of Goolsby (1971)

and T. Tom (1973).

b. Austenitizing Temperature and Hardenability

The foregoing discussion showed that using relatively high

austenitizing temperature dissolved a greater proportion of alloy carbides

and that this was usually associated with a large increase in prior

austenitic grain size. Both the above phenomena tend to increase

hardenability, i.e., either a thicker section can be through-hardened

for a given quenching rate, or, alternatively, a slower quenching rate

may be used for a given section size without encountering the usually

undesirable microstructural effects of metastable austenite decomposition.

Austenitizing temperatures higher than those conventionally employed may

therefore be used: (1) to enhance the hardenability of low alloy steels,

and (2) to promote the presence of desirable phases for enhanced fracture

toughness, such as retained austenite. An example of each of these

possibilities is discussed in the following section (see also Katz, 1961

and 1965).

The room temperature plane strain fracture toughness of a relatively

low hardenability steel, AISI 4130, is shown in Fig. 14 as a function of

tempering temperature for several austenitizing treatments. The

tempering response of this steel and others as a function of austenitizing

temperature is discussed in a subsequent section. The plane strain

fracture toughness of the as-quenched steel varies markedly with austenitizing

temperature and severity of quench. An austenitizing temperature of 1200°C

followed by an ice-brine quench and refrigeration in liquid nitrogen (IBQLN) resulted in nearly a two-fold increase in room temperature fracture toughness compared to that obtained by the conventionally recommended heat treatment of austenitizing at 870°C and oil quenching. A somewhat slower quench from 1200°C, i.e., oil quench vs. ice-brine, also improved the toughness relative to the commercial heat treatment but not so much as the more severe quench. Associated with the increases in fracture toughness were corresponding microstructural changes, as shown in Fig. 15 (a) and (b). The microstructure of a fracture toughness specimen oil quenched from 870°C consisted of a mixture of blocky ferrite and martensite, as shown in Fig. 15 (a). Extensive transmission electron microscopy using thin foils revealed that some of the martensite was autotempered. The microstructural appearance of a specimen ice-brine quenched from 1200°C was quite different, viz., there was virtually no evidence of ferrite, as shown in Fig. 15 (b). A similar correspondence between heat treatment, fracture toughness and microstructure existed for steel AISI 4330. Plots of plain strain fracture toughness vs. tempering temperature for two austenitizing treatments are shown in Fig. 16. Additional information on these steels is found in the investigations of Wood et al. (1973).

Unconventional heat treatments of the kind described above for steels of high hardenability resulted in similar improvements in fracture toughness even though there appeared to be no corresponding micro-structural changes except the expected grain size differences, as determined by optical metallographic observations. The room temperature plane strain fracture toughness of AISI 4340 steel is plotted in Fig. 17 as a function of tempering temperature for two austenitizing treatments. The

preferred heat treatment involves a step-quench from 1200°C to 870°C followed
by an oil quench.   Quench cracking occurred in the steel when it was
quenched from the higher temperature or if a quench more drastic
than oil was used.   As can be seen from Fig. 17 the plane strain fracture
toughness of the as-quenched steel was nearly doubled by the step-quench
heat treatment.   Examination of the microstructures by transmission
electron microscopy of specimens given both types of heat treatment
revealed differences in the amount of retained austenite and in the
nature of the substructure.   As shown in the bright and dark field
transmission micrographs of the specimen conventionally heat treated,
the amount of retained austenite (revealed by use of an austenite
reflection) was small, as shown in Fig. 18 (a) and (b).   In contrast,
the same metallographic technique revealed extensive networks of retained
austenite --- in some areas of the specimen almost every martensite plate
and lath was surrounded by austenite films that were 100-200 Å thick,
as shown in Fig. 19 (a) and (b).

Transmission electron microscopy revealed another distinct micro-
structural difference between specimens given the two heat treatments.
The packets of lath martensite were very similar for both austenitizing
treatments.   However, twinned martensite plates were observed in the
conventional treatment only; the use of the step-austenitizing treatment
apparently resulted in the virtual elimination of twinned martensite
plates, as shown in a comparison of Figs. 20 (a) and (b).   A detailed
discussion of the role of these various changes in the microstructure
and their possible effects on fracture toughness is found in a paper by

Lai et al. (1974). Briefly, it appears that both the presence of
retained austenite, especially in the observed morphology, and the absence
of twinned martensite plates favor the fracture toughness of specimens
given the step-austenitizing heat treatment. Webster (1968 and 1971)
and Antolovich et al. (1974) have suggested that retained austenite may
enhance the fracture toughness of high strength steels by either blunting
an advancing crack or by undergoing a strain- or stress-induced transformation
at the advancing crack tip. The consequences of the latter have been
considered by Gerberich et al. (1971) and Antolovich and Singh (1971),
as well as by Zackay et al. (1973). Das and Thomas (1969), Thomas (1971),
and Thomas and Das (1971) have comprehensively treated the problem of
twinned martensite plates as they influence the fracture toughness of
ultra-high strength steels. With the existing information, it is not
possible to establish the individual or combined role of these micro-
structural features on the fracture toughness of complex high strength
steels. The need for definitive solutions of these and other problems
in the design of new and superior steels is discussed in a later section.

c. Austenitizing Temperature and Tempering Response

In the foregoing discussion, attention was centered on the
effects that variations in the austenitizing temperature can have on
the plane strain fracture toughness of as-quenched steels. It was
shown that these effects, whether beneficial or detrimental, could usually
be traced to the appearance or disappearance of some element of micro-
structure or substructure. The same can be said of the tempering
response, although the causal relationships are less clear and are
dependent in some cases upon subtle combined chemical and mechanical
effects which appear to take place on a sub-microscopic scale.

The influence on tempering with variations in austenitizing temperature and severity of quench was shown earlier for several commercial steels, viz., Fig. 14 for AISI 4130 steel, Fig. 16 for AISI 4330 steel, and Fig. 17 for AISI 4340 steel. The chemical composition of these steels and one other --- the 300-M steel, are shown in Table III. The last mentioned steel is a modified version of AISI 4340 steel containing 0.08% vanadium and 1.59% silicon. A comparison of Figures 14, 16, and 17 reveal that the use of higher austenitizing temperatures resulted in tempered martensite embrittlement for the AISI 4130 and 4340 steels in tempering range of 200-350°C. This type of embrittlement was not observed for the AISI 4330 and 300-M steels treated at the high austenitizing temperature or for any of the steels conventionally heat treated. The fracture of the embrittled specimens was intergranular along prior austenite grain boundaries, while that of unembrittled specimens (either in the as-quenched condition or tempered at 200°C) occurred by dimpled rupture. No significant microstructural differences could be detected by transmission electron microscopy between the embrittled and the unembrittled specimens. The only compositional difference between the embrittled and unembrittled steels was the presence of vanadium in the latter. Several possible causes of the observed change in fracture mode have been discussed in detail by Lai et al. (1974). One of the possible mechanisms for this type of embrittlement is the presence of certain impurity elements as suggested by Capus and Mayer (1960), Low (1969), Kula and Anctil (1969), and Ohtani et al. (1974), among others. Kula and Anctil suggest that when cementite grows at prior austenite grain boundaries during tempering, such impurity elements as phosphorus, which are probably more soluble in

ferrite than in cementite, will diffuse out of the cementite into the
surrounding ferrite.   A film of segregated impurities might build up
at the interface between ferrite and cementite.   The presence of the
film may then result in a lowering of the interfacial energy and provide
a low-energy path for intergranular fracture.   Ohtani et al. (1974) have
suggested a similar mechanism for temper embrittlement.   These workers
contend that the classic equilibrium segregation theory of temper
embrittlement may have to be discarded.   In accordance with their model,
stabilization of carbides by elements such as molybdenum or vanadium is
a possible way of suppressing embrittlement.   The experimental results
presented in this section on the tempering response of vanadium-containing
and vanadium-free commercial steels subjected to high austenitizing
temperatures are therefore not inconsistent with the Kula and Anctil
model for tempered martensite embrittlement.

Finally, no review of impurity effects on the toughness of high
strength steels should exclude mention of the deleterious influences of
sulfur and phosphorus.   A recent representative study in this field was
that of Birkle et al.   (1966), who examined the relationship between
the density and distribution of sulfide inclusions and plane strain
fracture toughness.   The effect of the sulfur level on the fracture
toughness of 0.45C-Ni-Cr-Mo steels is shown in Fig. 21, from Birkle et al.,
(1966).   The authors conclude from fractographic studies that the crack
growth process consists of the growth and coalescence of voids nucleated
by sulfide inclusions and carbide particles.   The average spacings
between the sulfide inclusions decreased with increasing sulfur content
and correlated well with the "process zone" sizes computed using a model

by Krafft (1964) in which the onset of plane strain fracture instability
is related to the tensile plastic flow instability in a small zone of
material ahead of the crack tip.

In a study of the role of impurity elements (P, S, Cu, As, Sn) on
the critical flaw size for catastrophic fracture, Cottrell (1970) stressed
the importance of the synergistic influence of impurities. For example,
the combined effect of As and S in degrading fracture toughness was far
greater than the sum of their individual effects. As might be expected,
the most serious deterioration of toughness was observed at a tempering
temperature when both temper embrittlement (dependent on tempering temperature)
and sulfide embrittlement (largeley independent of tempering temperature)
occurred.

It may be concluded from these few representative studies that
impurity levels and types have major influences on the plane strain
fracture toughness of ultra-high strength steels. As Cottrell points
out in his paper, the effect of purification on the critical defect size,
in a conventional low alloy steel with a yield strength of 240,000 psi,
may be far greater than that achieved by the alternative route of the
substitution of the low alloy steel with a maraging steel. Darmara
(1967) has reviewed some then current and proposed methods of purifying
steel. It is clear from his remarks and from the continuing high level
of activity in this area that the steel-making processes of the future
will produce steels with combinations of mechanical properties that are
achieved now only in the controlled purity alloys of the research laboratory.

C. An Important Unsolved Problem

The alloying elements of steel and the solid state reactions which
they undergo determine the structure and, therefore, the properties of
steel. The complex nature of these reactions is not yet fully
understood and an understanding of the nature of these reactions important
in the economic design of superior steels. For example, even if the
influences of all the common alloying elements were individually known
on the thermodynamics and kinetics of the principal isothermal reactions
of plain carbon steels, the information would be insufficient for the
effective design of complex steels because commercial steels contain
many interacting elements whose total effect is often different from
that predicted on the basis of the individual elements alone. A real
need exists therefore for a technique for rapidly predicting the single
and the combined effects of all the common alloying elements on the
solid state metallurgical reactions that are important in the heat
treatment of steel. Knowing the initiation (incubation) and finish
times of these reactions and their associated kinetics is particularly
important. Progress made in the authors' laboratory in developing
such a technique is described below.

The rapid method of studying the isothermal reactions in steels
consists in quenching the steel sample from the austenitizing temperature
to a subcritical temperature in an isothermal bath and holding it within
the magnetic field of an inductor coil. The increase in permeability
accompanying austenite decomposition increases the inductance of the ooil,
and this changes the resonant frequency of the circuit. An automatic
continuous recording of the corresponding period provides a convenient

and accurate method for following the austenite decomposition. Quantitative information on austenite decomposition kinetics can be obtained within two seconds after the start of quenching (Babu et al., 1973; and Ericsson et al., 1974). An example illustrating some of the preliminary results obtained by this method is described below.

In the recently reported T-T-T diagrams for AISI 4340 steel, the bainite range is shown as a smooth C-shaped curve, Fig. 22 (a). Investigations by the new method showed significant differences in the shape and character of the lower bainite region. As shown in Fig. 22 (b), the incubation period for the formation of lower bainite decreased at temperatures just above M_s and gave an S-shaped curve for the bainite reaction. This acceleration of austenite decomposition at temperatures just above M_s has been observed previously (Howard and Cohen, 1948; Schaaber, 1955; and Radcliffe and Rollason, 1959).

That part of the lower bainite curve which extended below the M_s had a C-shape, as shown in Fig. 22 (b). Immediately below the M_s, the bainite reaction began almost instantly after the end of the martensite reaction. This rapid onset at temperatures just below the M_s is well established in the literature and is associated with the increased nucleation of the bainite reaction by the strain effects associated with the austenite to martensite transformation. The decreased rate of bainite formation at temperatures well below the M_s was apparently due to the lower diffusion rates of carbon.

Reactions of the type described above and their associated microstructures have meaning for both the user of existing commerical steels and the designer of new ones. To the user of commercial steels,

the precise location and shape of the lower and upper bainite reaction curves is significant from a hardenability viewpoint. Avoiding certain cooling rates can prevent the formation of upper bainite, an undesirable microstructure for mechanical properties. This is especially important in complex parts with varying section sizes. To the designer of new steels, knowledge of the details of the lower bainite and martensite reactions presents an opportunity to evaluate the mechanical properties of steels with the unusual mixed microstructures of lower bainite, autotempered and tempered martensite, and retained austenite. It is hoped that this new experimental technique for the rapid determination of T-T-T diagrams, coupled with basic studies of austenite decomposition on simplerhigh purity steels such as those, for example, of Aaronson and Domian (1966) and Hehemann et al. (1972), will eventually provide the basis for designing complex steels that are both economical and superior in properties to those currently available.

ACKNOWLEDGMENTS:

References

Aaronson, H. I., and Domian, H.A. (1966).   Trans. Met. Soc. AIME, 236,

  781-796.

Angel, T. (1954).   J. Iron Steel Inst., 177, 165-174.

Antolovich, S. D. (1968) Trans. Met Soc. AIME, 242, 2371-2373.

Antolovich, S. D. and Singh, B. (1971). Met. Trans., 2, 2135-2141.

Antolovich S. D.,Saxena, A., and Chanani, G. R. (1974). Met. Trans., 5,

  623-632.

Averback, B. L. (1968). In "Fracture" (H. Liebowitz, ed.), Vol. I,

  pp. 441-472, Academic Press, New York.

Babu, B. N. P., Ott, D. ,Parker, E. R., and Zackay, V. F. (1973).

  LBL-2502, In preparation, Lawrence Berkeley Laboratory, Berkeley, California.

Bhandarkar, D., Zackay, V. F., and Parker, E. R. (1972). Met. Trans., 3,

  2619-2631.

Birkle, A. J., Wei, R. P., and Pellissier, G. E. (1966). Trans. ASM, 59,

  981-990.

Bressanelli, J. P., and Moskowitz, A. (1966). Trans. ASM, 59, 223-239.

Capus, J. M., and Mayer, G. (1960). Metallurgia, 62, 133-138.

References contd.

Cottrell, C. L. M. (1970). In "Fracture Toughness of High Strength

Materials: Theory and Practice," ISI Publication 120, p. 112-115,

The Iron and Steel Institute, London.

Darmara, F. N. (1967). J. Metals, 19 (12), 42-48.

Das, S. K., and Thomas G. (1969). Trans. ASM, 62, 659-676.

Dokko, C. (1969). M. S. Thesis, UCRL-19068, University of California,

Berkeley, California.

Ericsson, C. E., Parker, E. R., and Zackay, V. F. (1974). In preparation,

Lawrence Berkeley Laboratory, Berkeley, California.

Fahr, D. (1969). Ph.D. Thesis, UCRL-19060, University of California,

Berkeley, California.

Fahr, D. (1971). Met. Trans., 2, 1883-1892.

Gerberich, W. W., and Birat, J. P. (1971). Int. J. Fract. Mech., 7, 108-110.

Gerberich, W. W., Hemmings, P. L.,Merz, M. D., and Zackay, V. F. (1968).

Trans. ASM, 61, 843-847.

Gerberich, W. W., Hemmings, P. L., Zackay, V. F., and Parker, E. R. (1969).

In "Fracture 1969" (P. L. Pratt, ed.), pp. 288-305, Chapman and Hall,

Ltd., London.

References contd.

-33-

Gerberich, W. W., Thomas G., Parker, E. R., and Zackay, V. F. (1970).

In Proc. 2nd Int. Conf. Strength of Metals and Alloys, Asilomar,

California, 1970, 3, 894-899.

Gerberich, W. W.,Hemmings, P. L., and Zackay, V. F. (1971). Met. Trans.,

2, 2243-2253.

Goolsby, R. D. (1971). Ph.D. Thesis, LBL-405, University of California,

Berkeley, California.

Hehemann, R. F.,Kinsman, K. R., and Aaronson, H. I. (1972). Met. Trans.,

3, 1077-1094.

Horwood, W. A. (1972). M.S. Thesis, LBL-1121, University of California,

Berkeley, California.

Howard, R. T., Jr., and Cohen, M. (1948). Trans. AIME, 176, 384-397.

Jin, S., Horwood, W. A., Morris, J. W., Jr., and Zackay, V. F. (1973a).

Advan. Cryog. Eng. In press.

Jin, S. , Morris, J. W., Jr., and Zackay, V. F. (1973 b). Advan. Cryog.

Eng. In press.

Jin, S., Morris, J. W., Jr., and Zackay, V. F. (1973 c). Presented at

Materials Engineering Congress, Chicago, Illinois, October 1973.

Katz, R. N. (1961), Tech. Note WAL TN 320.1/8, Watertown Arsenal,

Watertown, Mass.

Katz, R. N. (1965).   Tech. Note AMRA TN 65-09, Materials Engineering

Division, U. S. Army Materials Research Agency, Watertown, Mass.

Knott, J. F. (1973).   "Fundamentals of Fracture Mechanics,"

Butterworths, London.

Krafft, J. M. (1964).   Appl. Mater. Res., 3, 88-101.

Kula, E. B. and Anctil, A. A. (1969). J. Mater. 4(4), 817-841.

Kulin, S. A. Cohen, M., and Averback, B. L. (1952).   Trans.

AIME, 194, 661-668.

Lai, G. Y., Wood, W. E., Parker, E. R., and Zackay, V. F. (1974).   In

preparation.

Liebowitz, H. (1968), ed. "Fracture," Vol. I-VII, Academic Press, New York.

Loss, F. J. and Pellini, W. S. (1969). In "Practical Fracture Mechanics

for Structural Steel," Paper J, UKAEA, Chapman and Hall, London.

Low, J. R., Jr. (1969).   Trans. Met. Soc. AIME, 245, 2481-2494.

Ohtani, H., Geng, H. C., and McMahon, C. J., Jr. (1974).   Met. Trans., 5,

516-518.

Osborn, C. J., Gifkins, R. C., Hoggart, J. S., and Mansell, D. S. (1969),

eds. "Fracture," Proc. 2nd Tewksbury Symp., Fac. Eng. Univ. Melbourne,

Melbourne, Australia.

Pellini, W. S. (1968).   NRL Report 6713, April 3,   Naval Research

Laboratory, Washington, D.C.   Also, Welding Research Council Bulletin,

130, May 1968.

Puzak, P. P., and Lange, E. A. (1969).   NRL Rep. 6951, Sept. 18,

Naval Research Laboratory, Washington, D.C.

Radcliffe, S. V., and Rollason, E. C. (1959).   J. Iron Steel Inst.,

191, 56-65.

Sasaki, G. (1973).   D. Eng. Thesis, LBL-1493, University of California,

Berkeley, California.

Sasaki, G. Yokota, M. J., and Zackay, V. F. (1974).   In preparation,

Lawrence Berkeley Laboratory, Berkeley, California.

Schaaber, O. (1955).   Trans. AIME, 203, 559-560.

Scheil, E. (1932).   Z. Anorg. Allg. Chem., 207, 21-40.

Tamura, I., Maki, T., Hato, H., Tomoto, Y., and Akada, M. (1970).   In

Proc. 2nd Int. Conf. Strength of Metals and Alloys, Asimolar, California

1970, 3, 900-904.

Tetelman, A. S., and McEvily, A. J., Jr. (1967).   "Fracture of Structural

Materials," John Wiley and Sons, Inc., New York.

Thomas, G. (1971).   Met. Trans., 2, 2373-2385.

Thomas G., and Das, S. K. (1971).   J. Iron Steel Inst., 209, 801-804.

Tom, T. (1973), D. Eng Thesis, LBL-1856, University of California,

Berkeley, California.

Webster, D. (1968).   Trans. ASM, 61, 816-828.

Webster, D. (1971).   Met. Trans., 2, 2097-2104.

Wood, W. E., Parker, E. R., and Zackay, V. F. (1973).   LBL-1474,

Lawrence Berkeley Laboratory, Berkeley, California.

Yakota, M. J., Sasaki, G., Horwood, W. A., Zackay, V.F., and Parker, E. R.,

(1974 a).   LBL-2278, in preparation, Lawrence Berkeley Laboratory,

Berkeley, California.

Zackay, V. F., Parker, E. R., Fahr, D., and Busch, R. (1967).   Trans. ASM,

60, 252-259.

Zackay, V. F. (1973).   In "Microstructure and Design of Alloys," pp. 591-595,

Institute of Metals, London.

TABLE I

CHEMICAL COMPOSITIONS OF TRIP STEELS

Designations	Compositions, Wt.%			
	C	Ni	Cr	Mn
CN8Cr	0.325	8.0	9.0	2.0
CN12Cr	0.290	12.0	9.0	2.0
CN16Cr	0.292	16.0	9.0	2.0
CN21Cr	0.287	21.4	9.0	2.0

TABLE II

CHEMICAL COMPOSITIONS OF C-Mo STEELS

Designations	Compositions, Wt.%					
	C	Mo	Ni	Mn	S	P
0.34C-1Mo	0.34	0.95	----	0.63	0.005	0.008
0.30C-2Mo	0.32	1.96	---	0.65	0.005	0.007
0.30C-5Mo	0.30	5.03	---	0.60	0.005	0.008
0.41C-5Mo	0.41	4.93	----	0.51	0.005	0.007
0.35C-1Mo-3Ni	0.35	0.95	3.1	0.61	0.005	0.007
0.35C-2Mo-3Ni	0.35	1.90	3.1	0.67	0.005	0.007

Sn, Sb < 0.002%, As < 0.005% and

Si < 0.02% in all steels.

TABLE III

CHEMICAL COMPOSITION OF LOW ALLOY STEELS

STEEL	Compositions, Wt.%									
	C	Mn	Cr	Ni	Mo	S	Si	Cu	P	V
AISI 4130-A	0.31	0.57	0.85	0.15	0.18	0.009	0.28	0.21	0.008	<0.005
AISI 4130-B	0.33	0.63	0.90	0.15	0.18	0.009	0.27	0.19	0.008	<0.005
AISI 4330	0.28	1.02	0.85	1.80	0.40	0.005	0.28	0.10	0.009	0.07
AISI 4340	0.40	0.85	0.72	1.73	0.26	0.010	0.22	0.14	0.004	<0.005
300-M	0.41	0.79	0.75	1.85	0.43	0.002	1.59	0.04	0.008	0.08

Figure Captions

Fig. 1. Plots of Charpy V-notch impact energy at -196°C vs. reheating temperature for Fe-12Ni-0.5Ti alloy. The heat treatments are indicated.

Fig. 2. Relationship between prior austenite grain size and Charpy impact energy at -196°C for the Fe-12Ni-0.5Ti alloy.

Fig. 3. The relation between engineering strain and the volume fraction of martensite that is produced in steel CN8Cr, deformed 70% at 450°C, when tested at a temperature of -78°C.

Fig. 4. The engineering stress-strain curves of steel CN8Cr, deformed 70% at 450°C (PDA is an abbreviation for prior deformation of austenite), tested at 22°C and -78°C. The values of the stability coefficient, m, are shown.

Fig. 5. The engineering stress-strain curves for steels containing 8, 12, and 16% nickel, deformed 70% at 450°C and tested at -78°C. The values of the stability coefficient, m, are shown.

Fig. 6. The correlation between the stability coefficient, m, and (a) the elongation to fracture, and (b) Lüders strain. Data were obtained from a large group of metastable austenitic steels of widely varying composition, processing histories, and testing temperatures.

Fig. 7. Influence of austenite stability (m value) on the plane stress fracture toughness of high strength metastable austenites.

Fig. 8. Effect of carbon and nitrogen contents on cleavage of martensite and hence on apparent K_{IC}, at -196°C.

Fig. 9. Influence of thickness on the critical stress intensity factors at room temperature for a TRIP steel and two commercial steels.

Fig. 10. Plots showing the influence of austenitizing temperature on room temperature fracture toughness (K_{IC} or K_Q), yield strength (Y.S.), and ultimate strength (U.S.) of 0.30C-5Mo and 0.41C-5Mo steels.

Fig. 11. Plots of room temperature plane strain fracture toughness vs. prior austenite grain size (indicated by ASTM grain size number) for as-quenched 0.34C-1Mo and 0.35C-1Mo-3Ni steels.

Fig. 12. Transmission electron micrograph of a carbon replica showing fine undissolved carbides in as-quenched 0.32C-2Mo steel, austenitized at 870°C.

Fig. 13. Transmission electron micrograph of a carbon replica showing 1-3 micron size undissolved carbides in as-quenched 0.30C-5Mo steel, austenitized at 870°C.

Fig. 14. Plots of room temperature plane strain fracture toughness vs. tempering temperature for AISI 4130 steel. Austenitizing temperatures and quenching media are indicated.

Fig. 15. Microstructure of AISI 4130 steel: (a) austenitized at 870°C and oil quenched (arrows indicate ferrite and upper bainite), and (b) austenitized at 1200°C and ice-brine quenched.

Fig. 16. Plots of room temperature plane strain fracture toughness vs. tempering temperature for AISI 4330 steel. Austenitizing temperatures and quenching media are indicated.

Fig. 17. Plots of room temperature plane strain fracture toughness vs. tempering temperature for AISI 4340 steel. Austenitizing temperatures and quenching media are indicated.

Fig. 18. Transmission electron micrographs of as-quenched AISI 4340
steel: (a) bright field and (b) dark field of austenite
reflection for the 870°C austenitized specimen.

Fig. 19. Transmission electron micrographs of as-quenched AISI 4340
steel: (a) bright field and (b) dark field of austenite
reflection for the 1200°C → 870°C austenitized specimen.

Fig. 20. Transmission electron micrographs of martensite plates in
AISI 4340 steel: (a) austenitized at 870°C, showing extensive
fine transformation twins in a martensite plate marked P,
(b) austenitized at 1200°C, showing absence of transformation
twins and presence of ε carbides in a cross-hatched morphology
in martensite plates marked P. A prior austenite grain boundary
is marked GB.

Fig. 21. Influence of sulfur level on plain strain fracture toughness
and strength of quenched and tempered 0.45C-Ni-Cr-Mo steels
(from Birkle et al., 1966).

Fig. 22. T-T-T diagrams of AISI 4340 steel: (a) as reported in the
literature, and (b) as determined by the new magnetic
permeability technique.
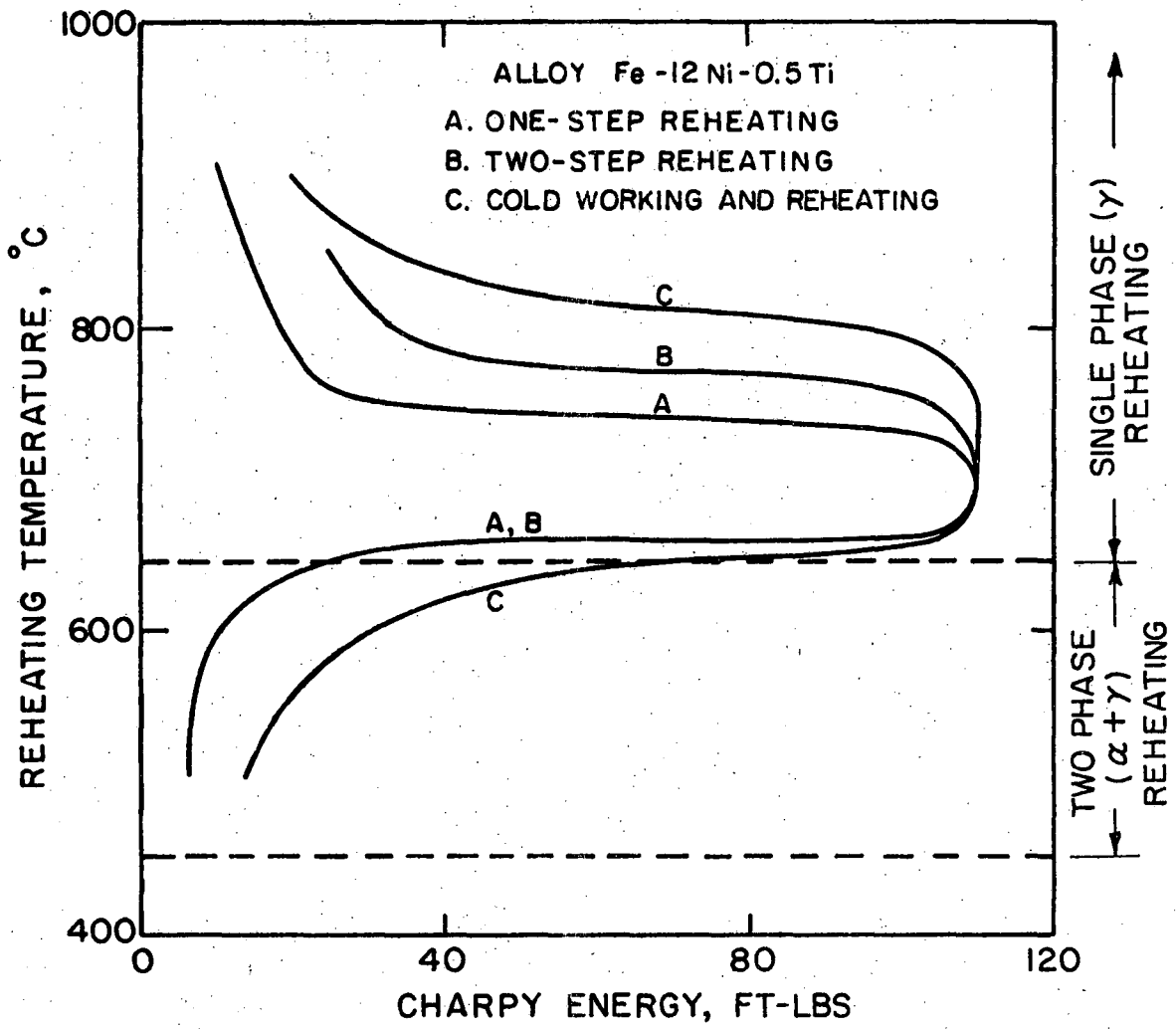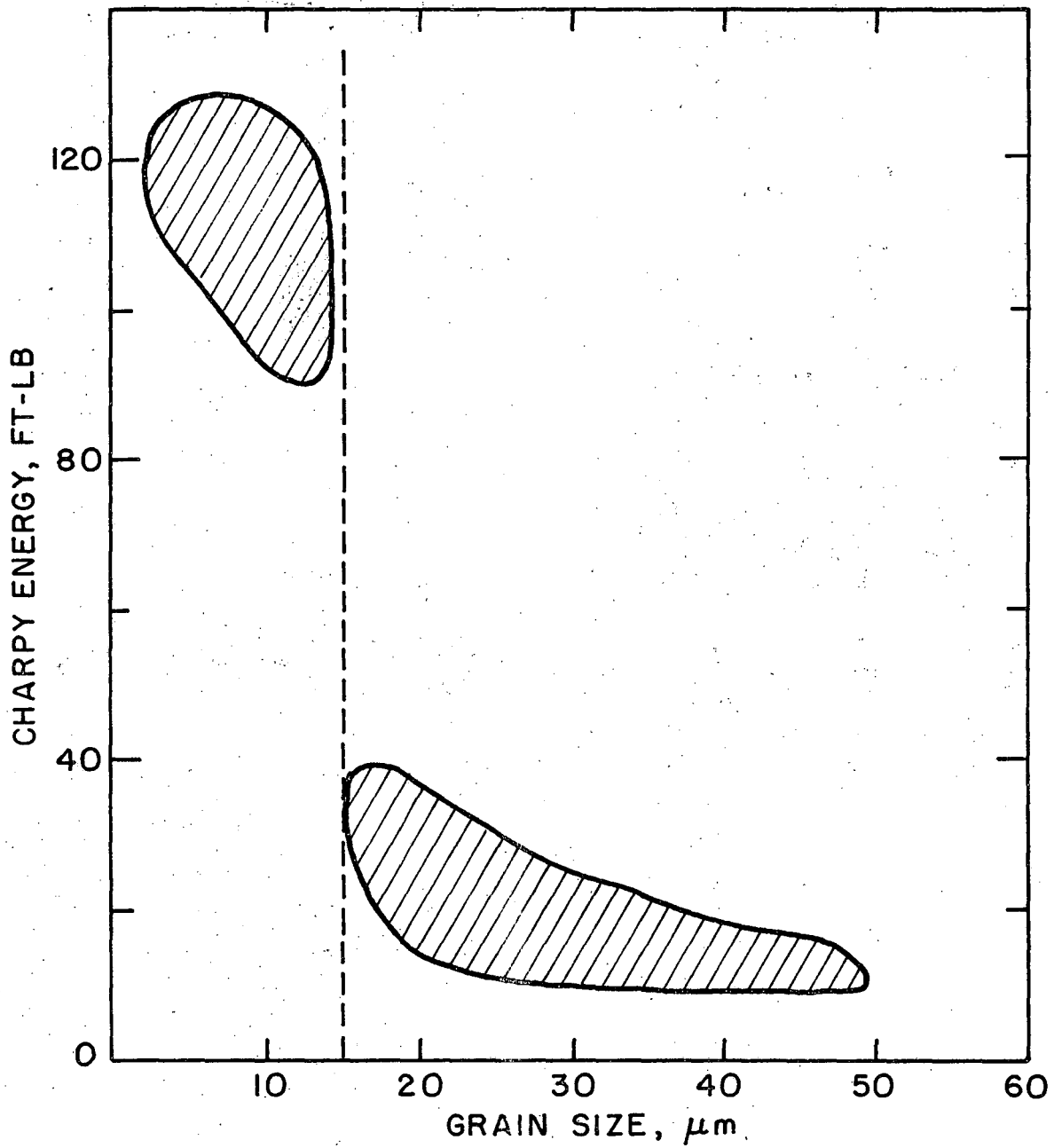
Fig. 1

XBL7311- 5599A

Fig. 2
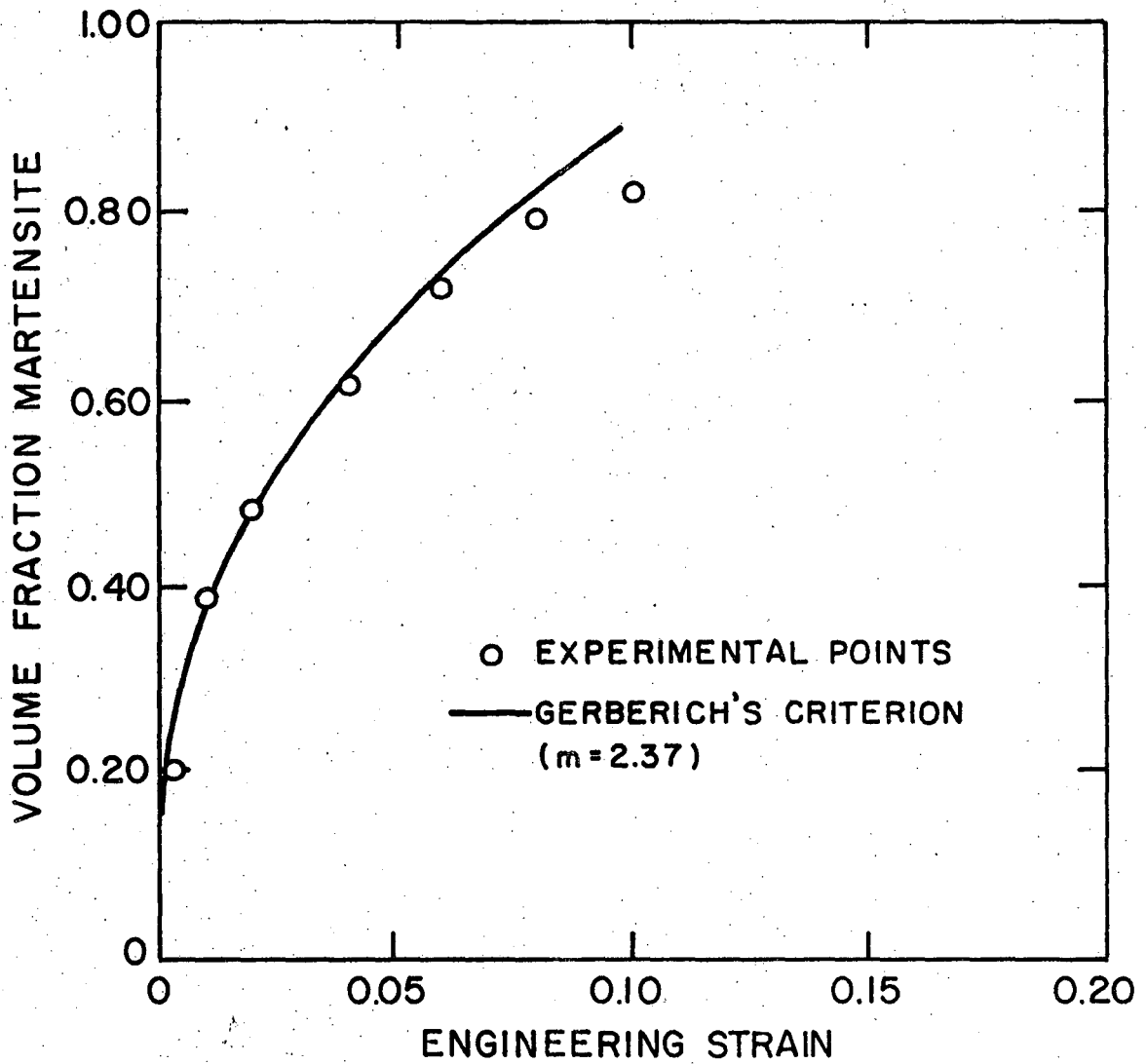
XBL 7110-7501A

Fig. 3
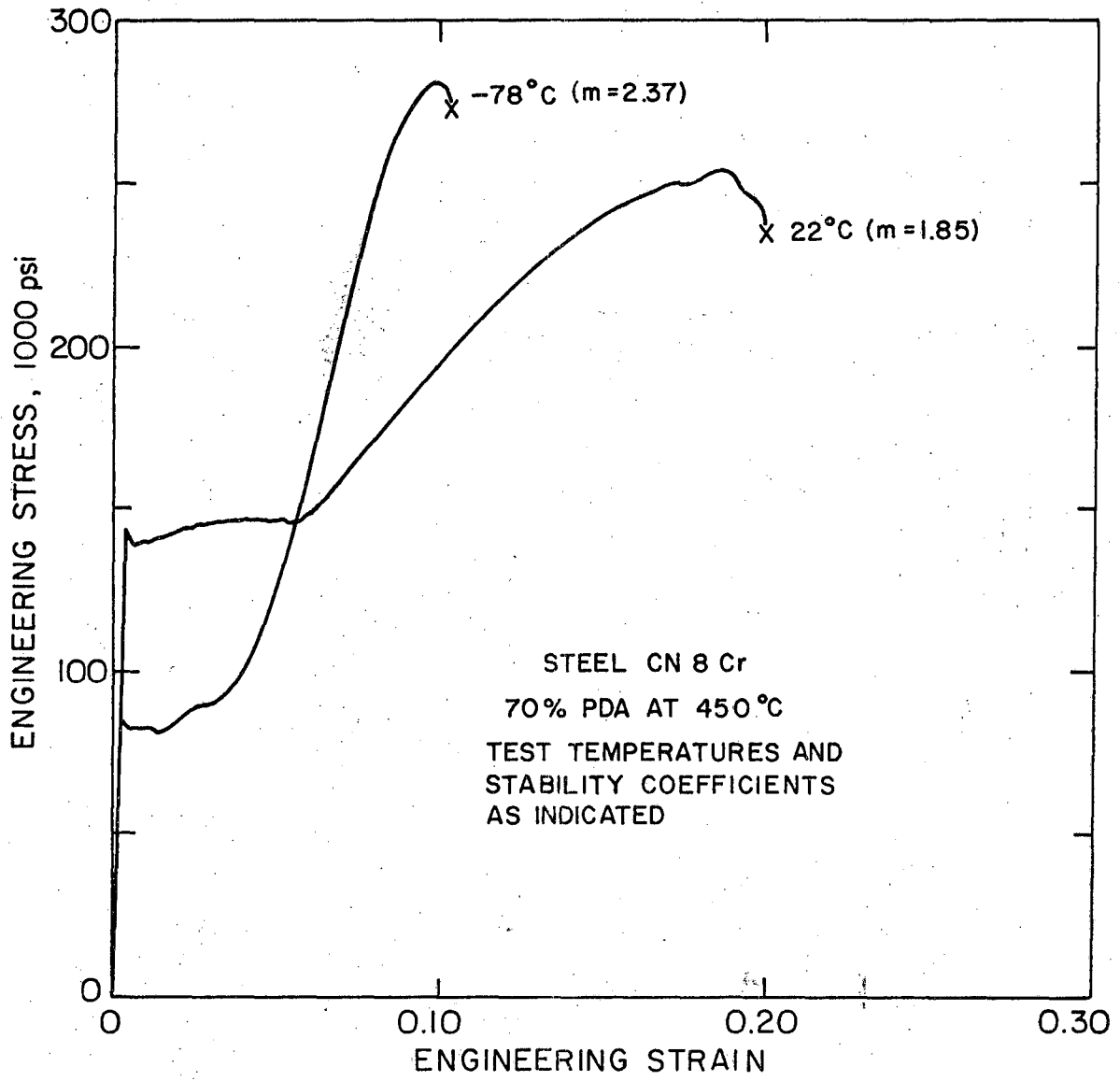
STEEL CN 8 Cr

70% PDA AT 450°C

TEST TEMPERATURES AND
STABILITY COEFFICIENTS
AS INDICATED

XBL 7110-7504A

Fig. 4

Fig. 5

XBL7III-7666A

Fig. 6(a)

XBL 7III-7662

Fig. 6(b)

XBL 7III-766I

Fig. 7

Fig. 8

XBL 701-210

O 9 Cr - 8 Ni - 4 Mo - 0.27C TRIP STEEL
σ_{YS} = 222 ksi

□ 4335 V-MOD. LOW ALLOY STEEL
σ_{YS} = 215 ksi

△ 13 Cr - 8 Ni - Mo PRECIPITATION HARDENED
STAINLESS STEEL
σ_{YS} = 200 ksi
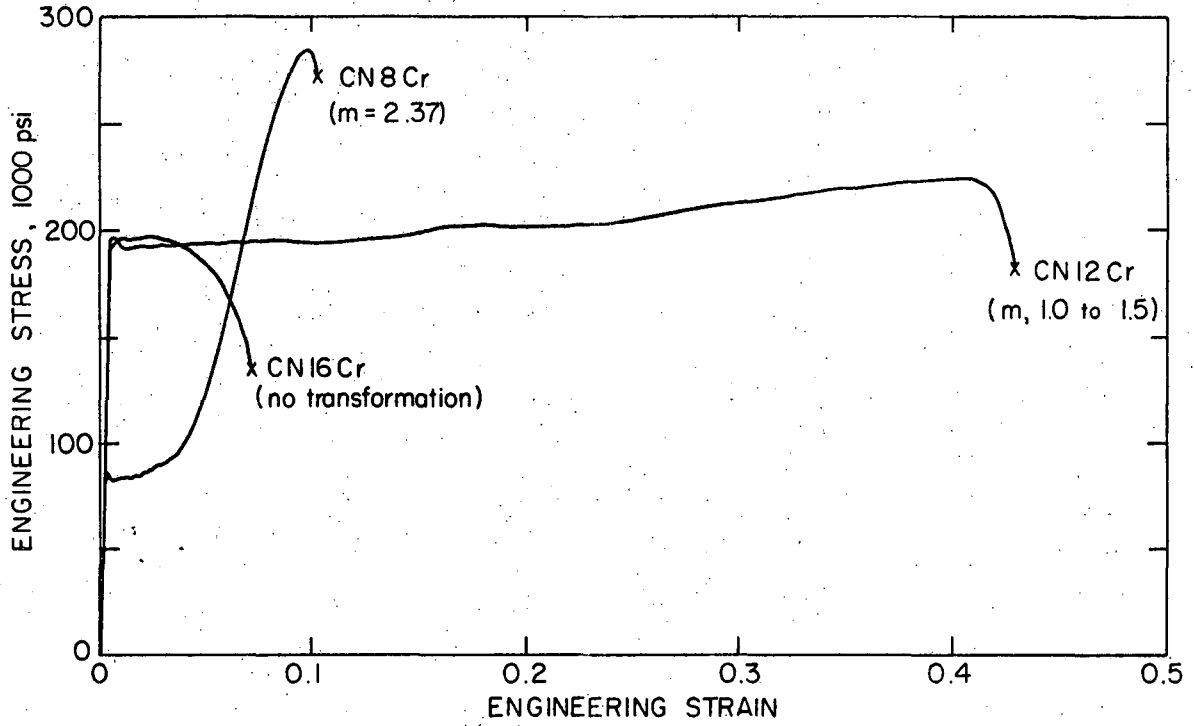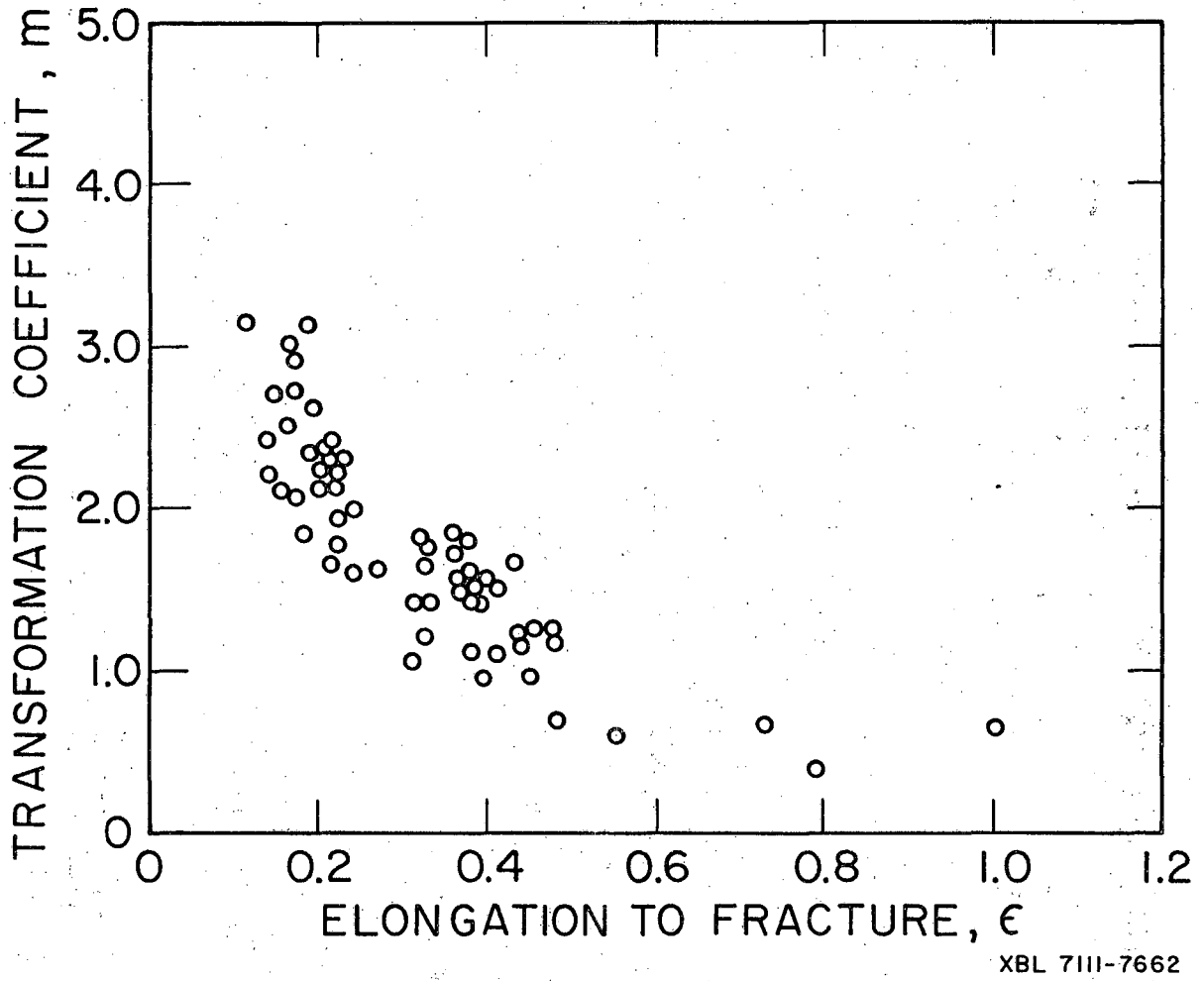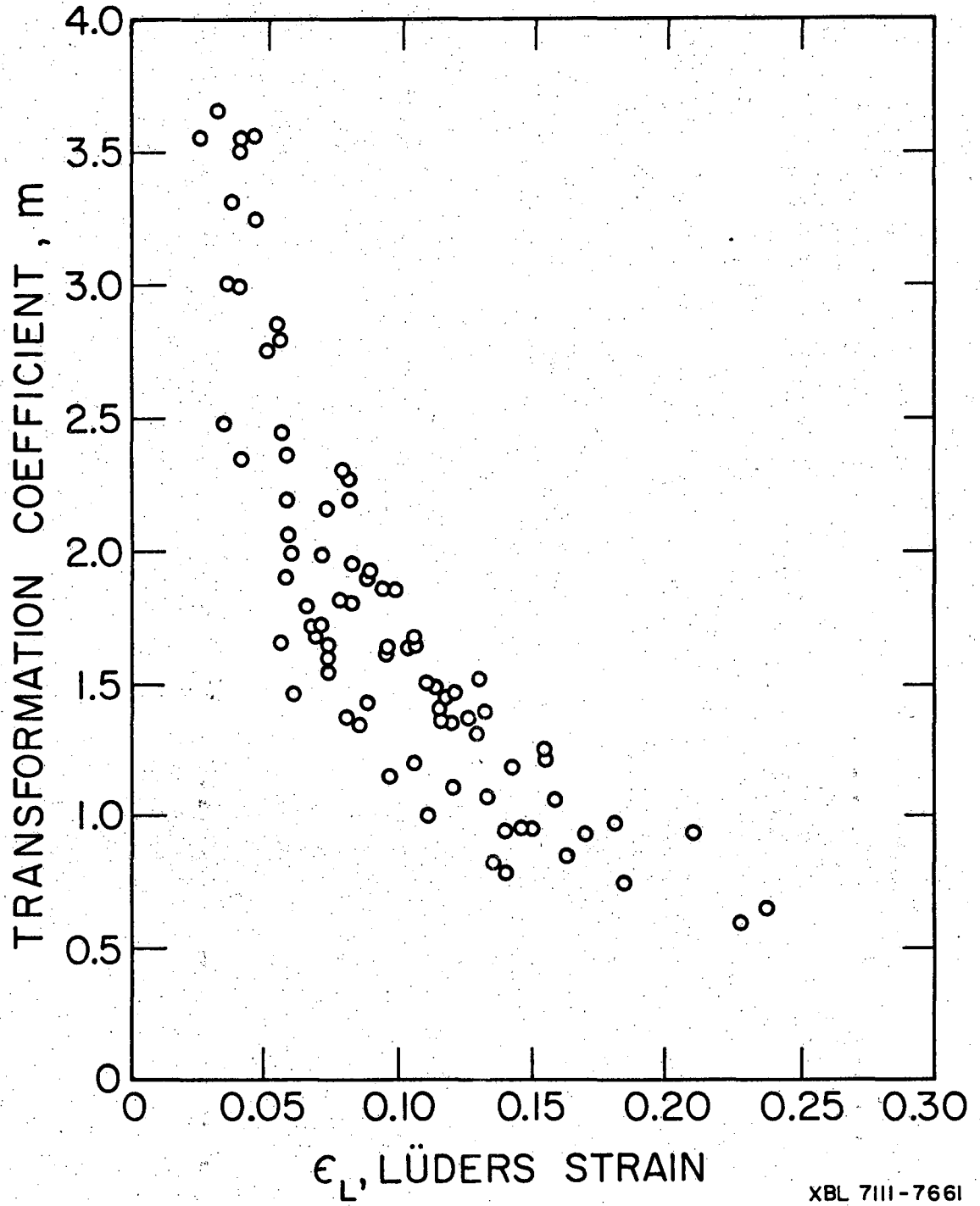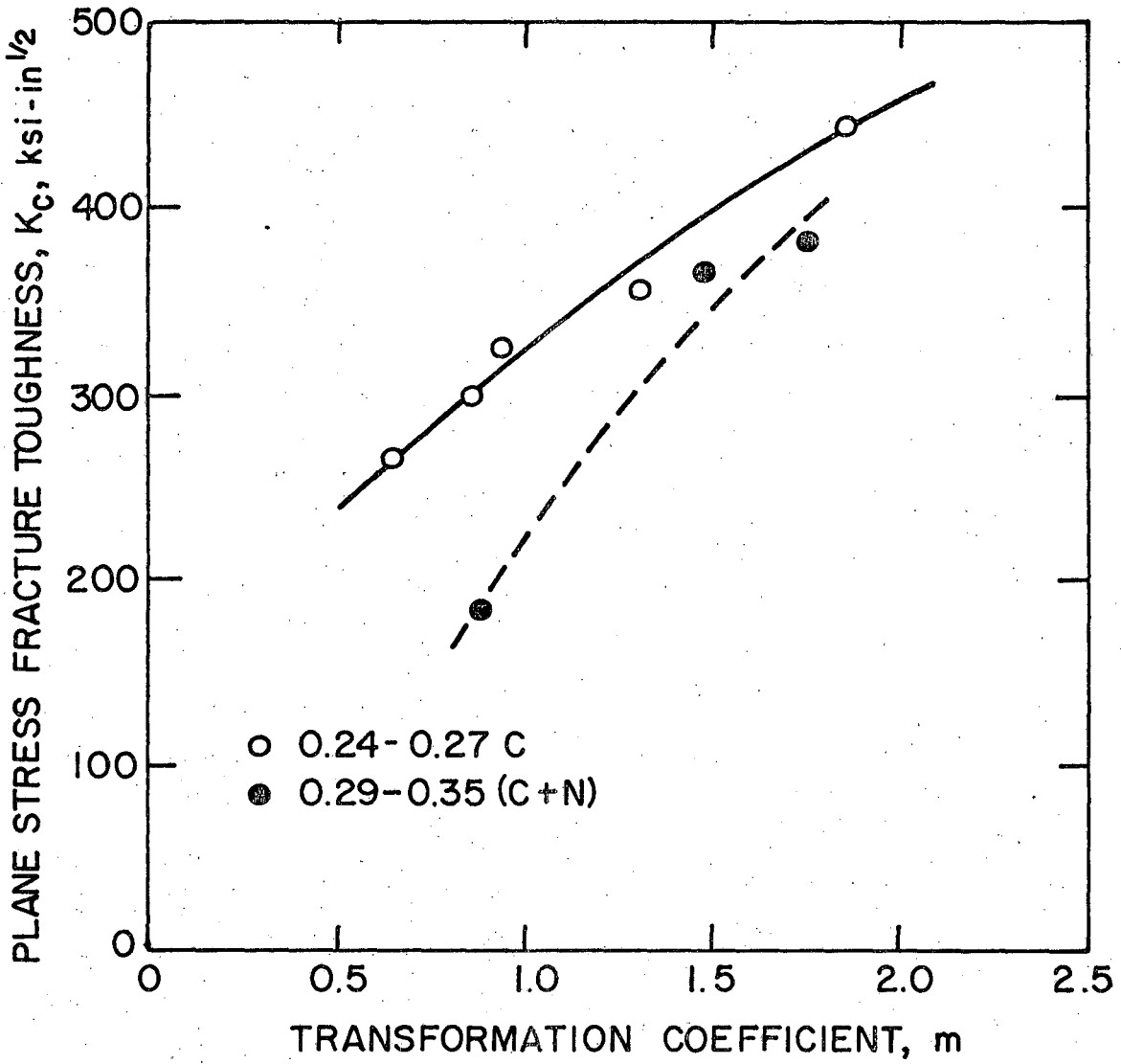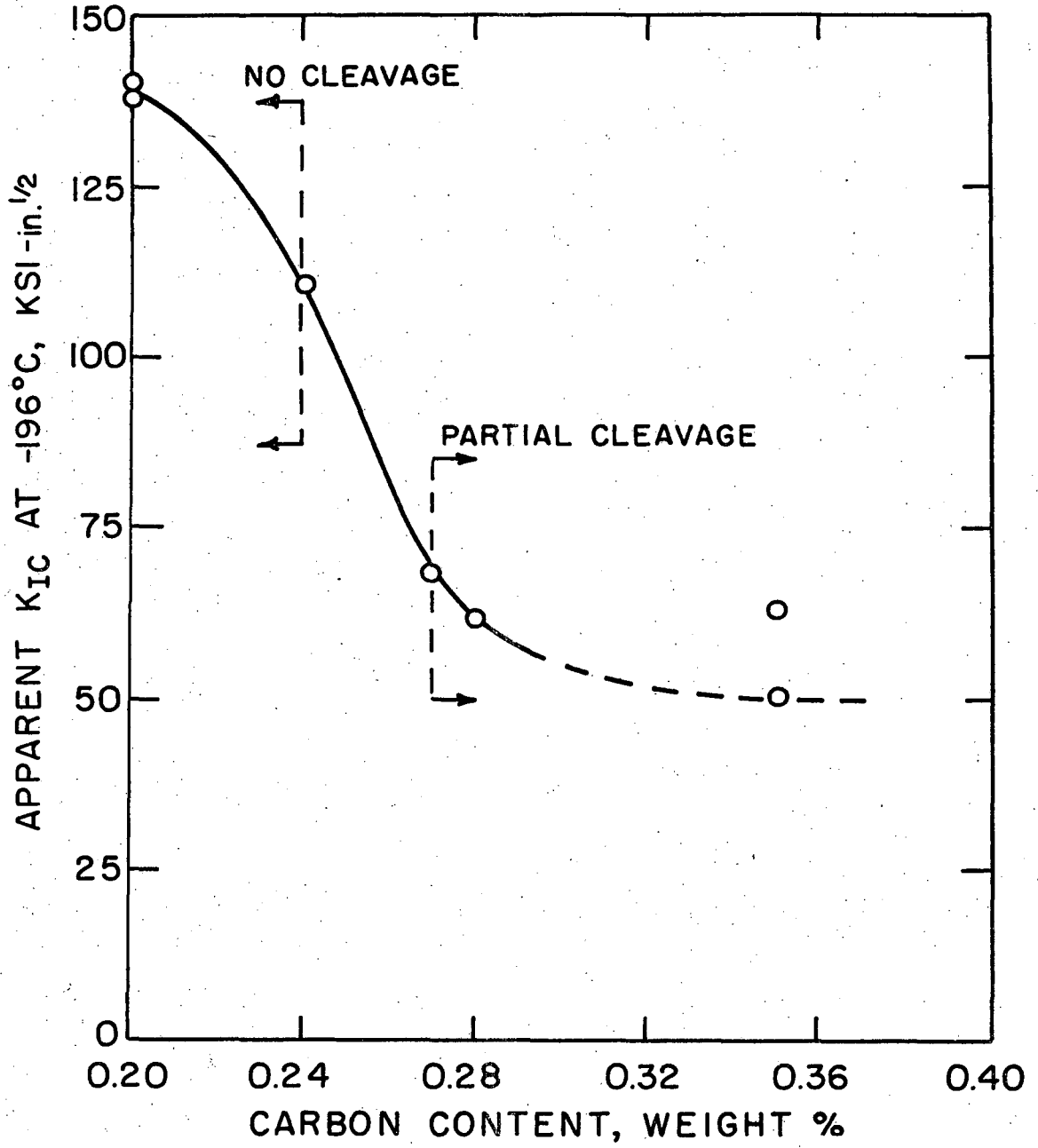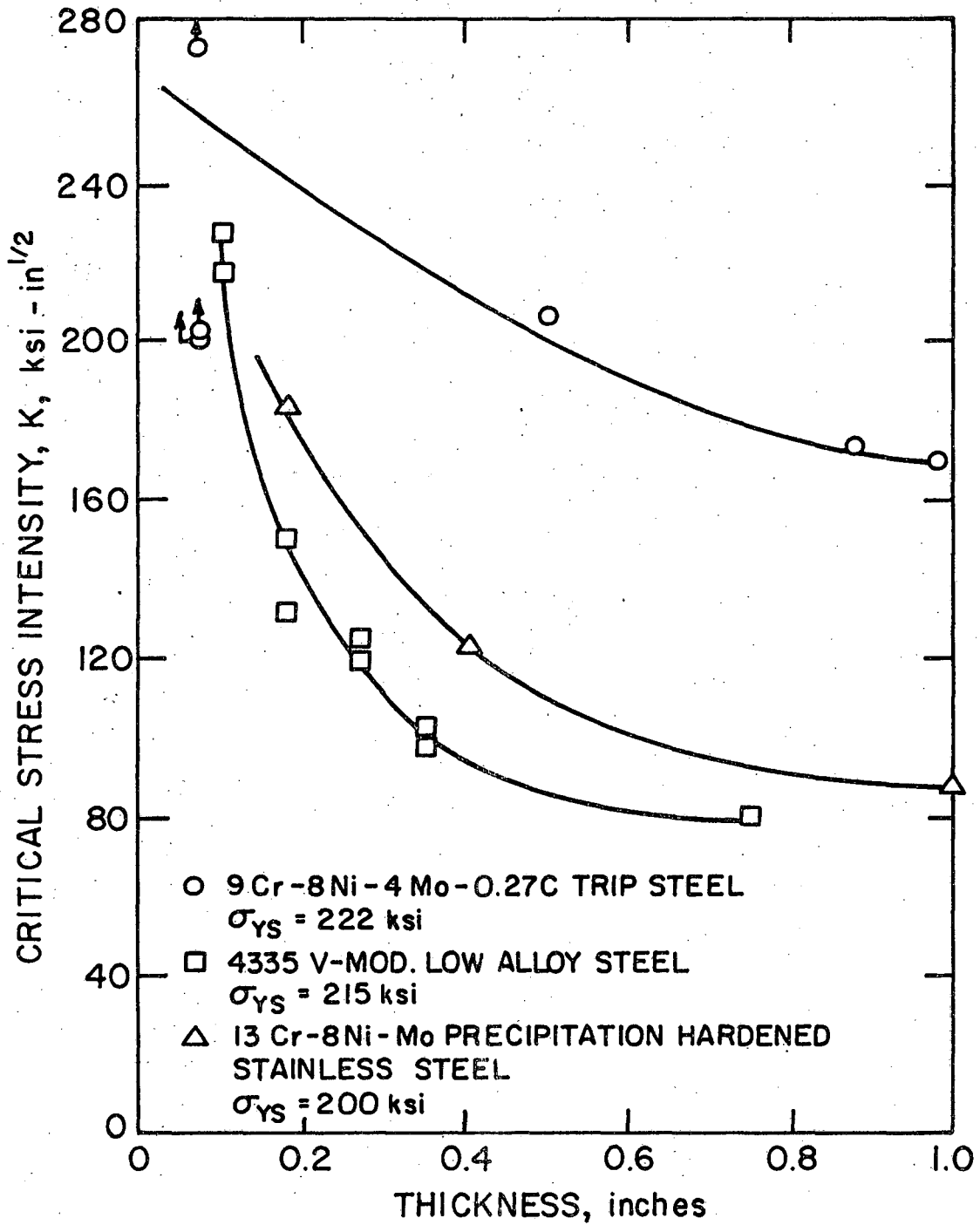
XBL 6811 - 6156A

Fig. 9
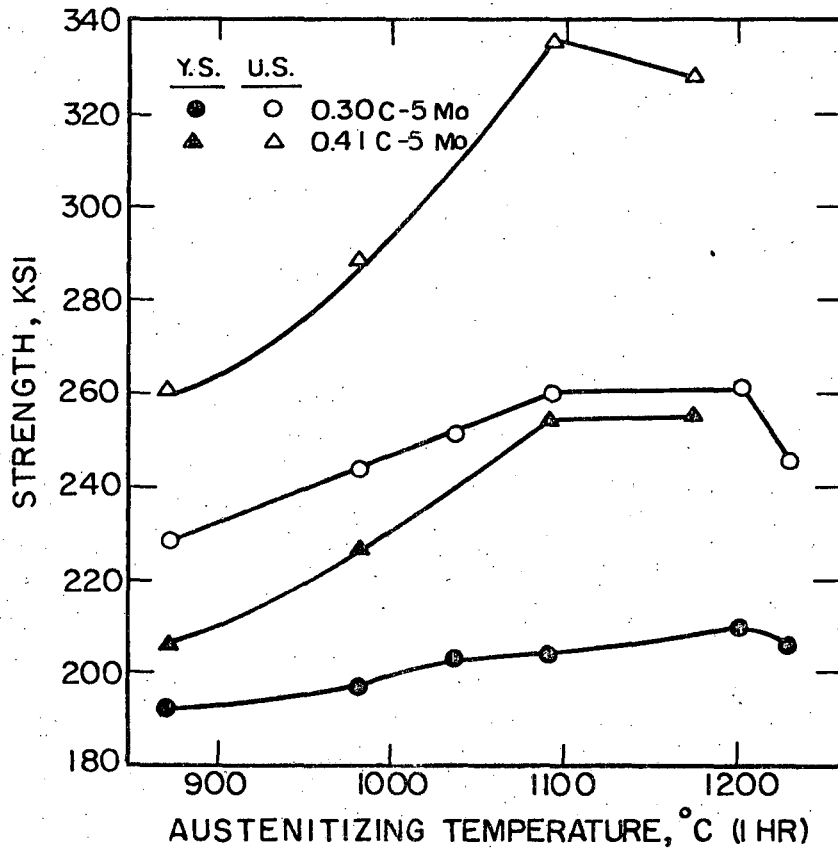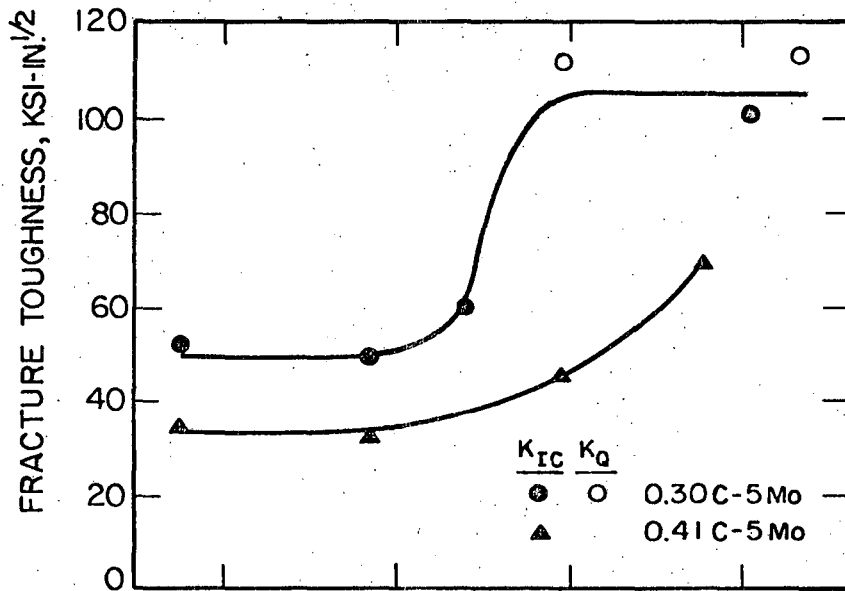
XBL737-6460A

Fig. 10

Fig. 11

2μ
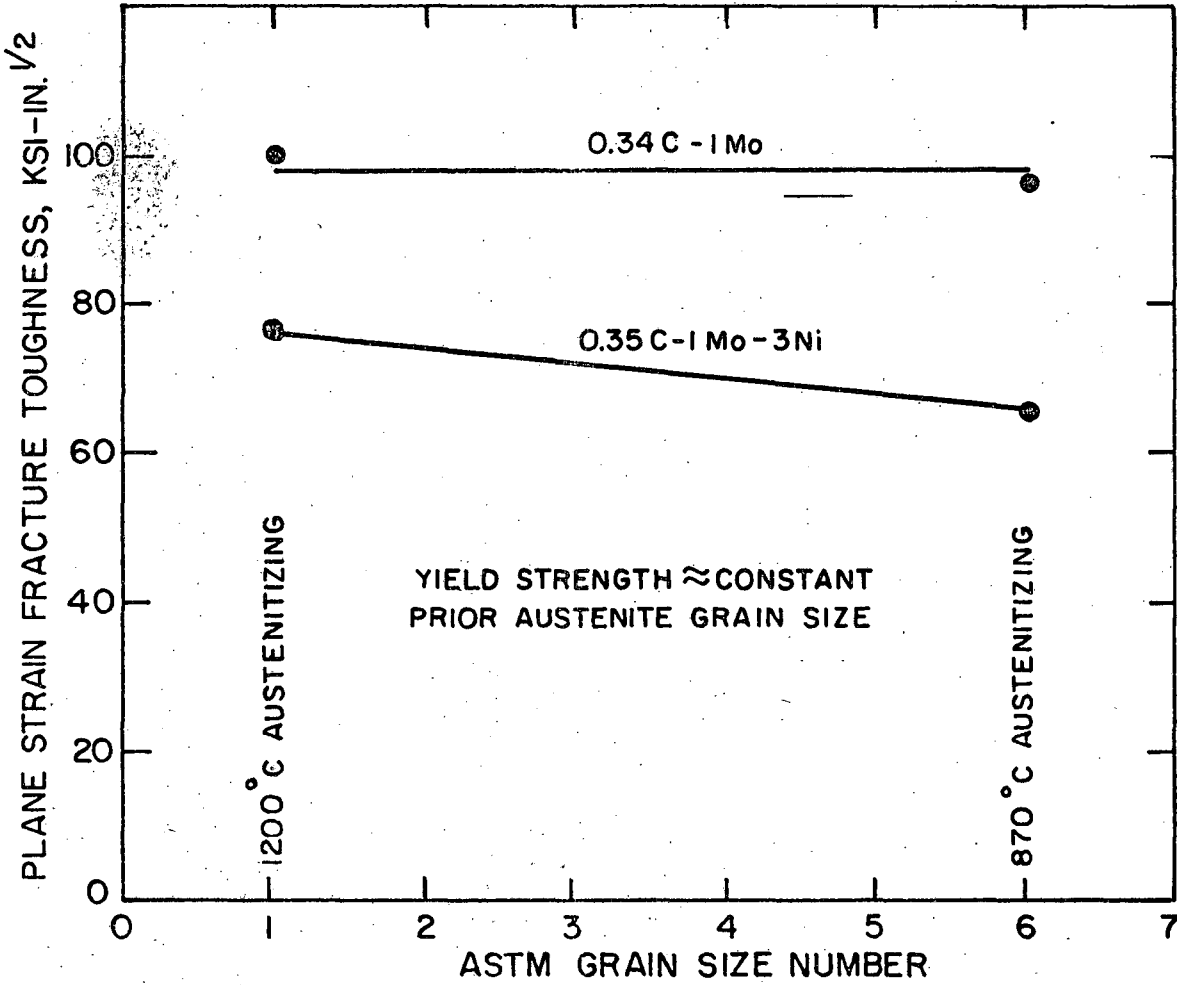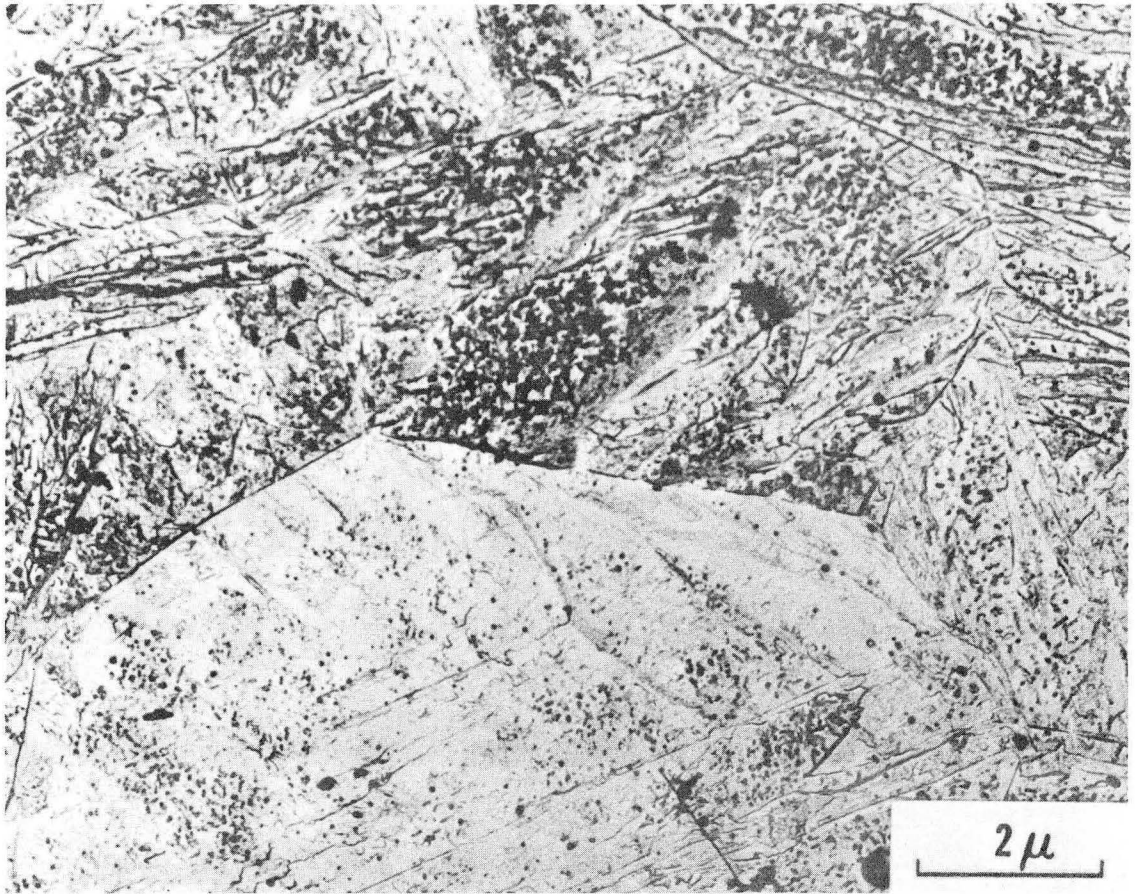
XBB 737-4410

Fig. 12
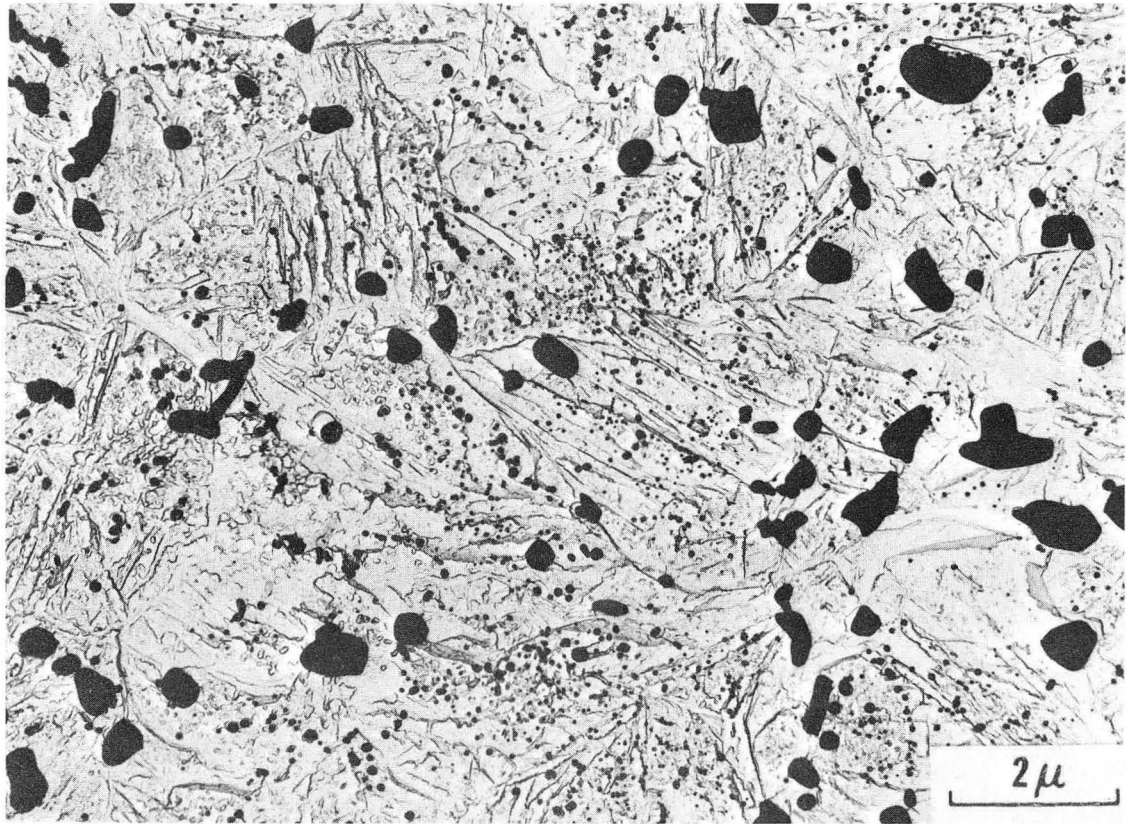
XBB 737-4407

Fig. 13
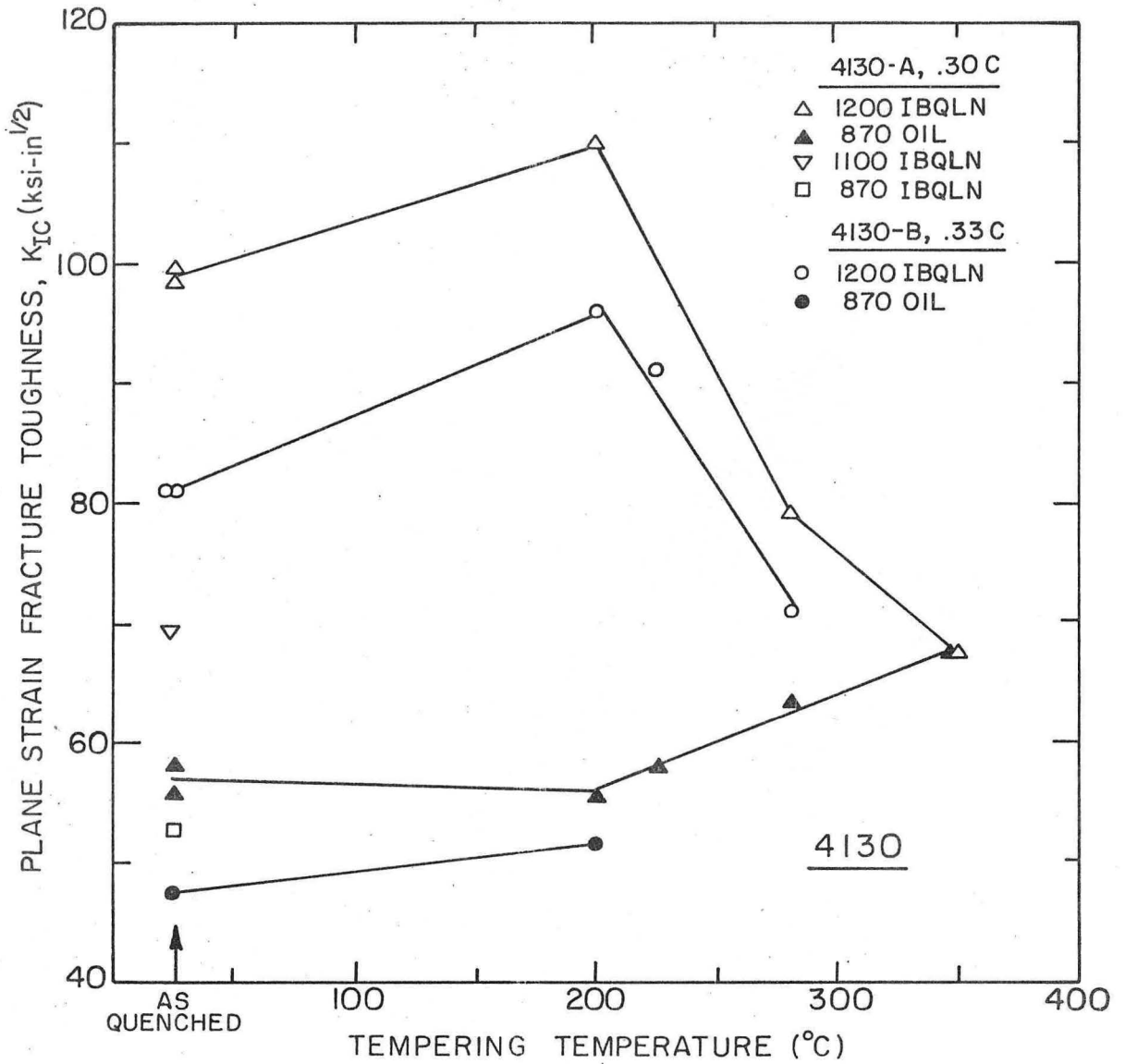
XBL 734-5971

Fig. 14

XBB 732-658

Fig. 15(a)

62 μ
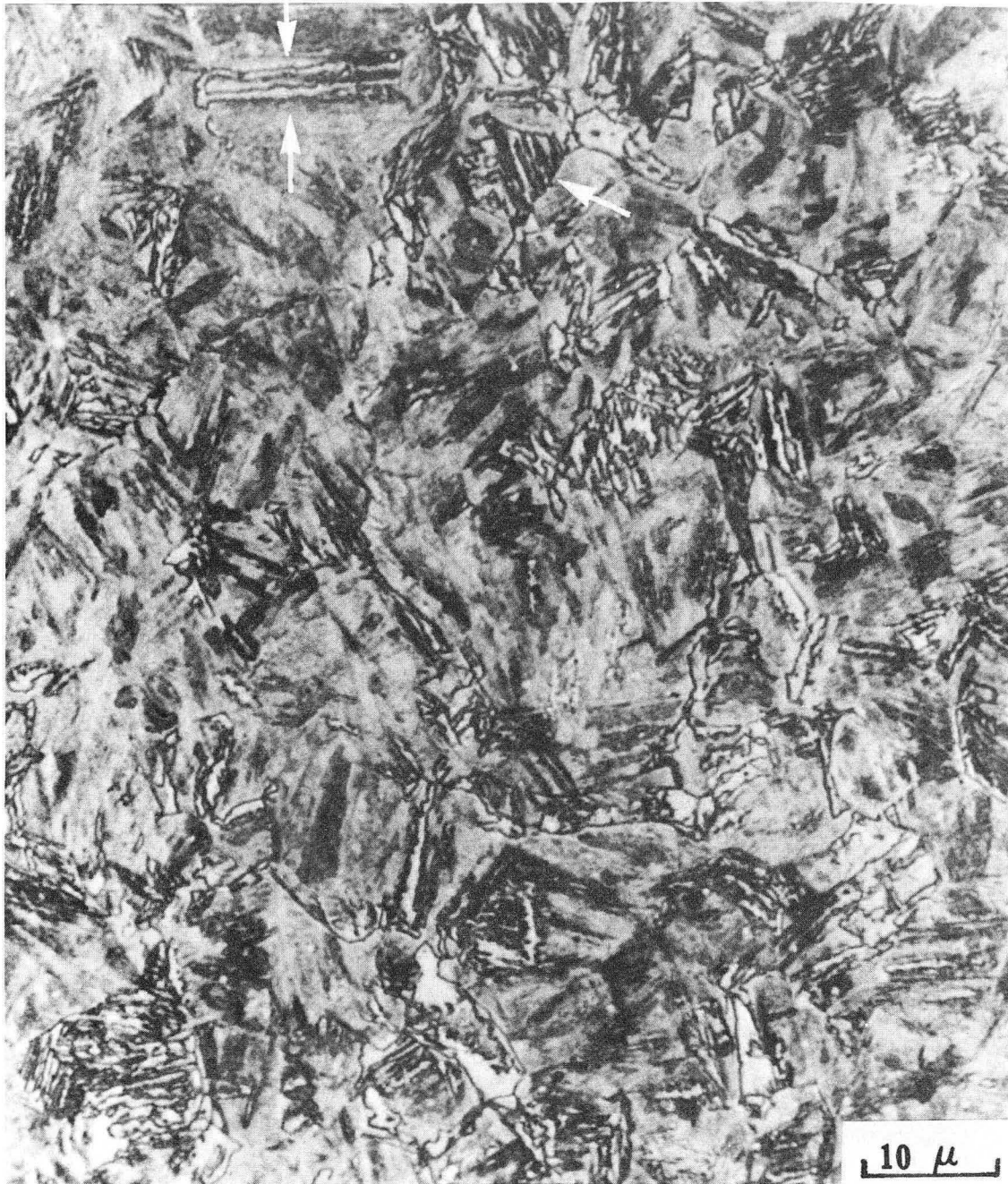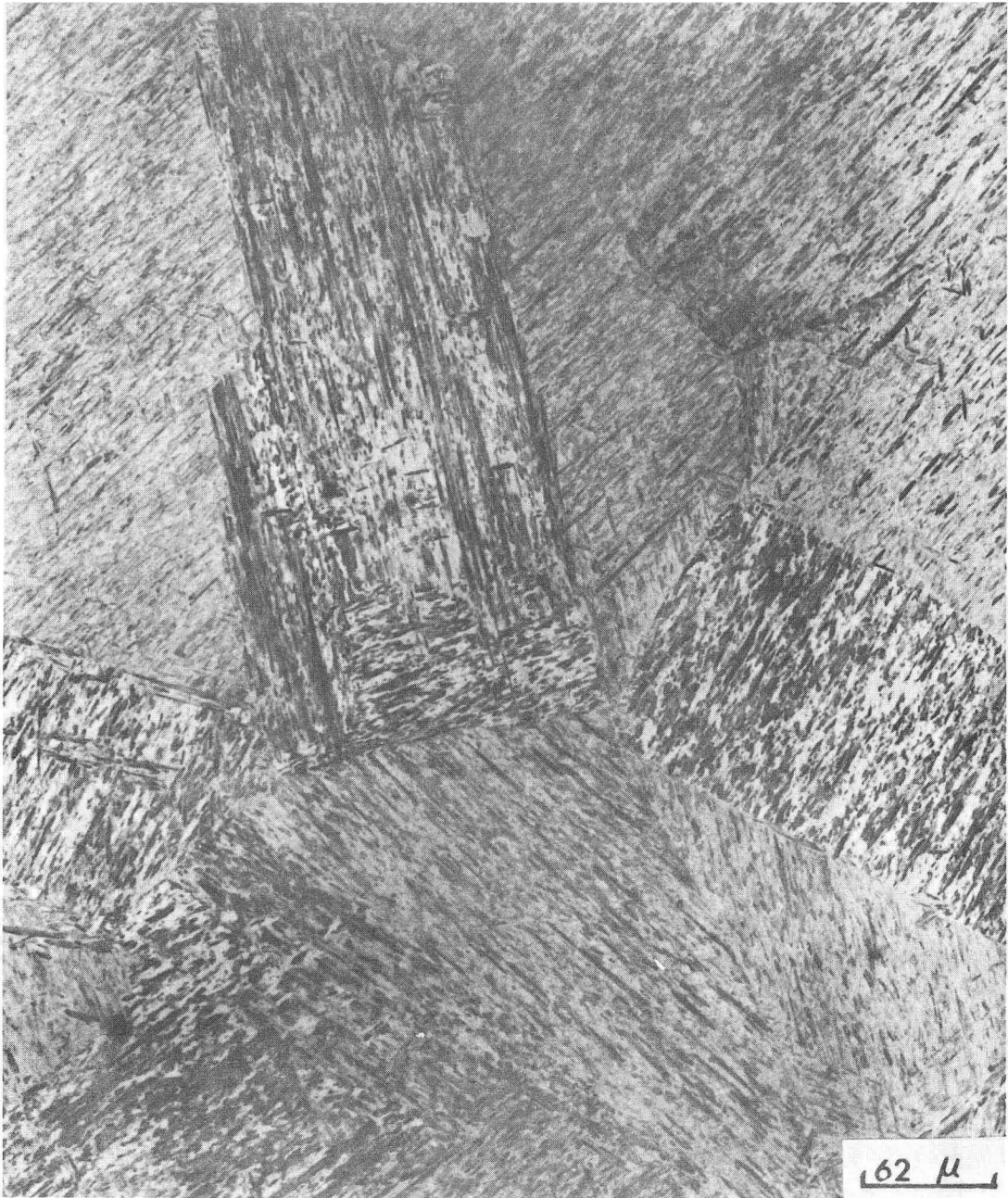
XBB 732-620

Fig. 15(b)
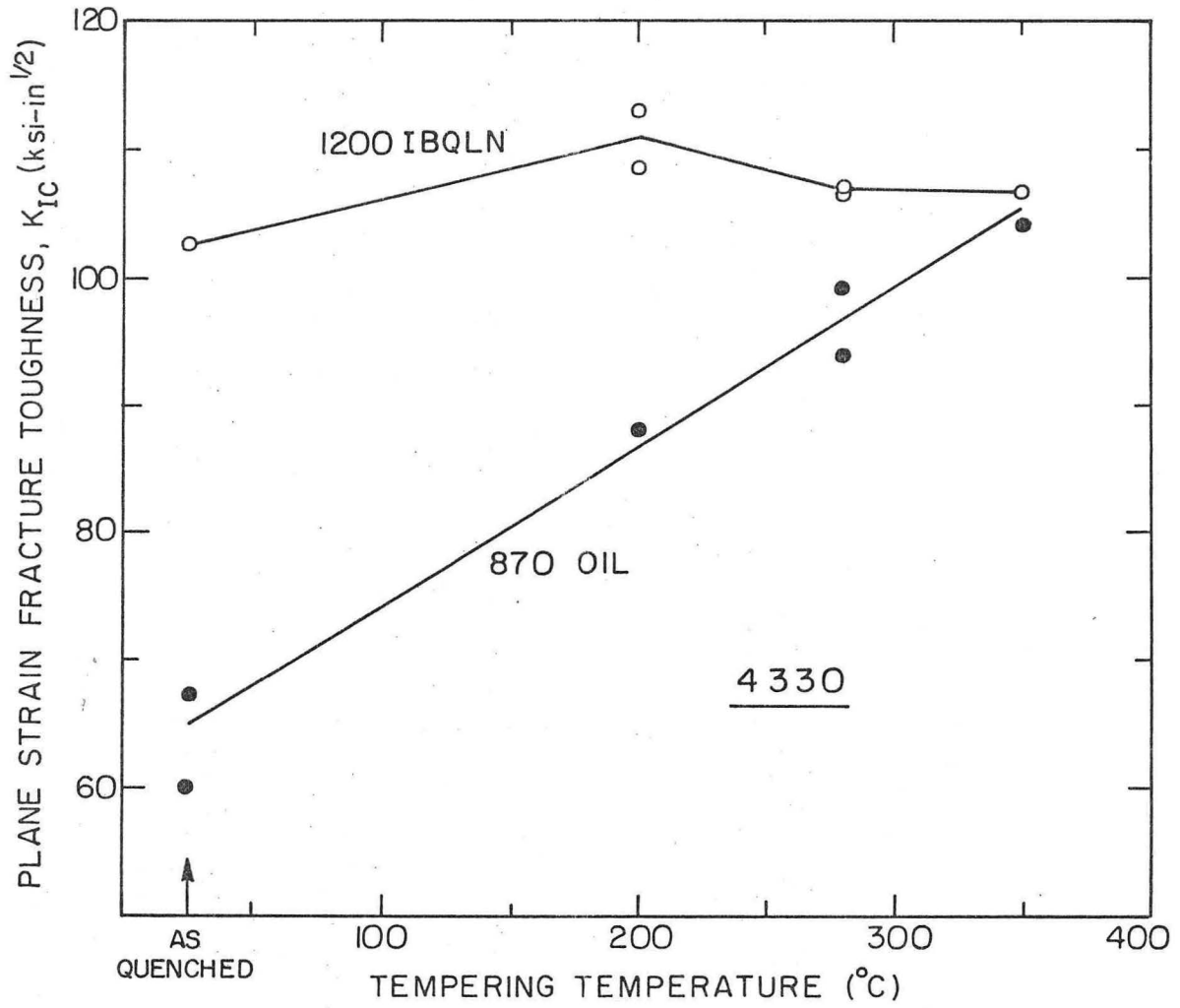
XBL 734-5973

Fig. 16
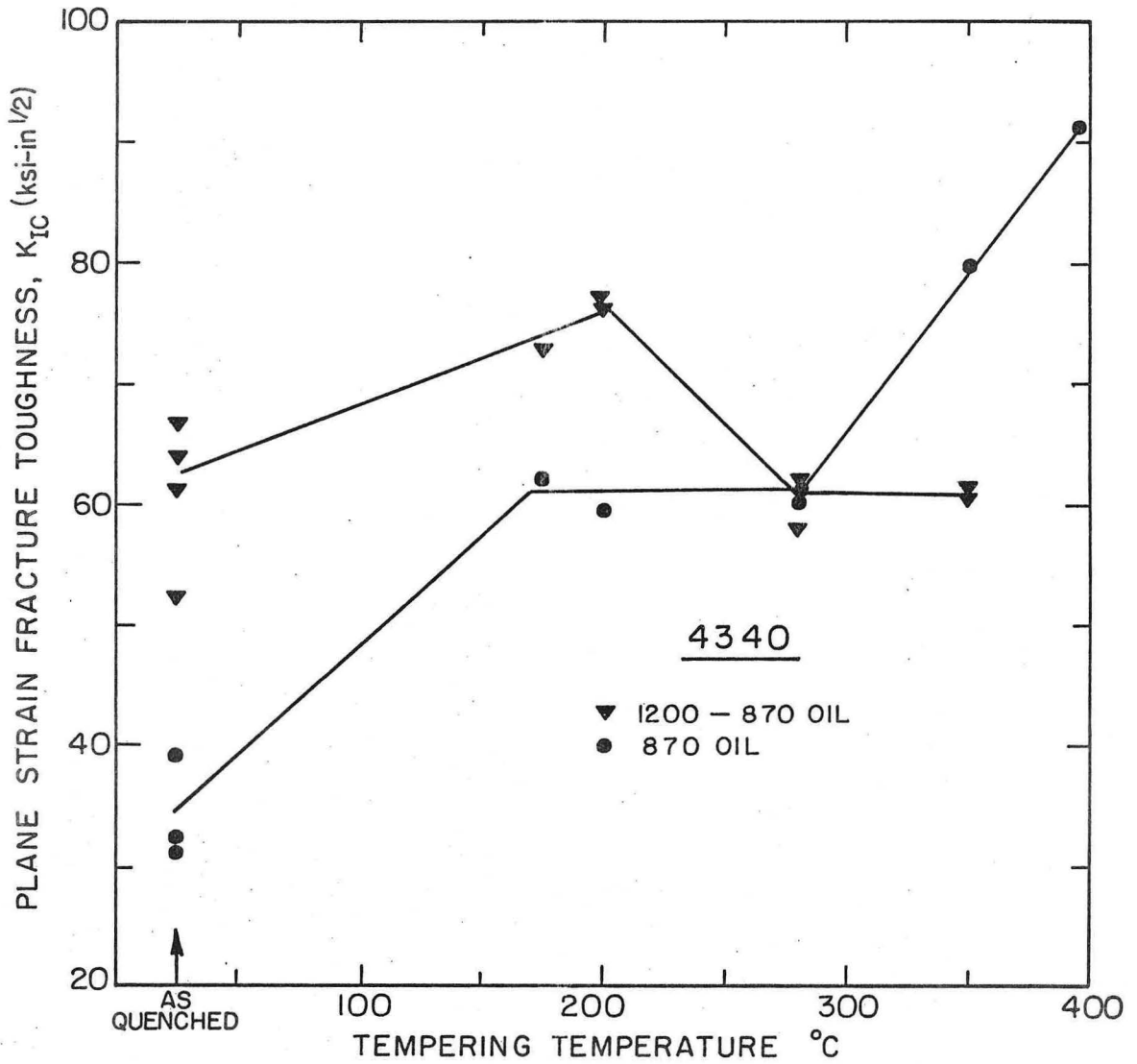
XBL734-5974

Fig. 17
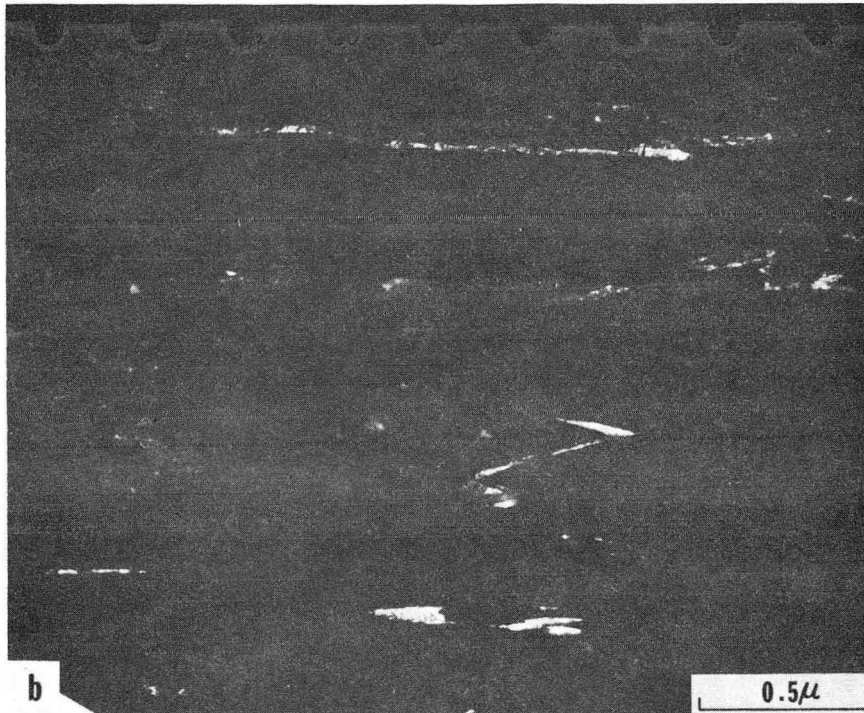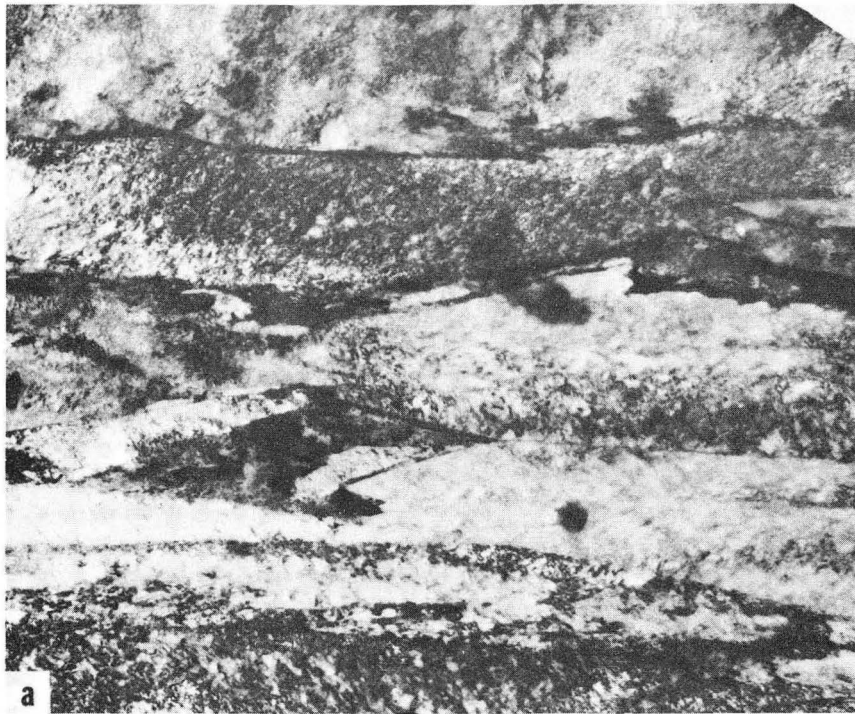
XBB 738-5026

Fig. 18
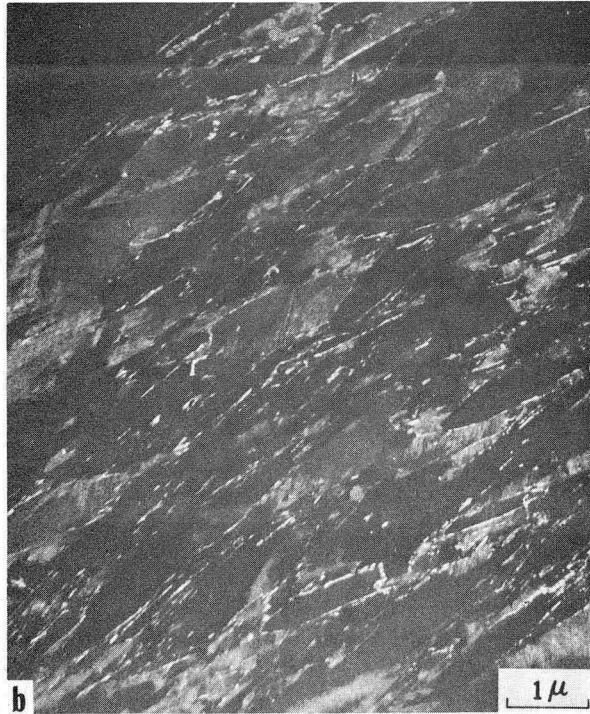
XBB 738-5025

Fig. 19
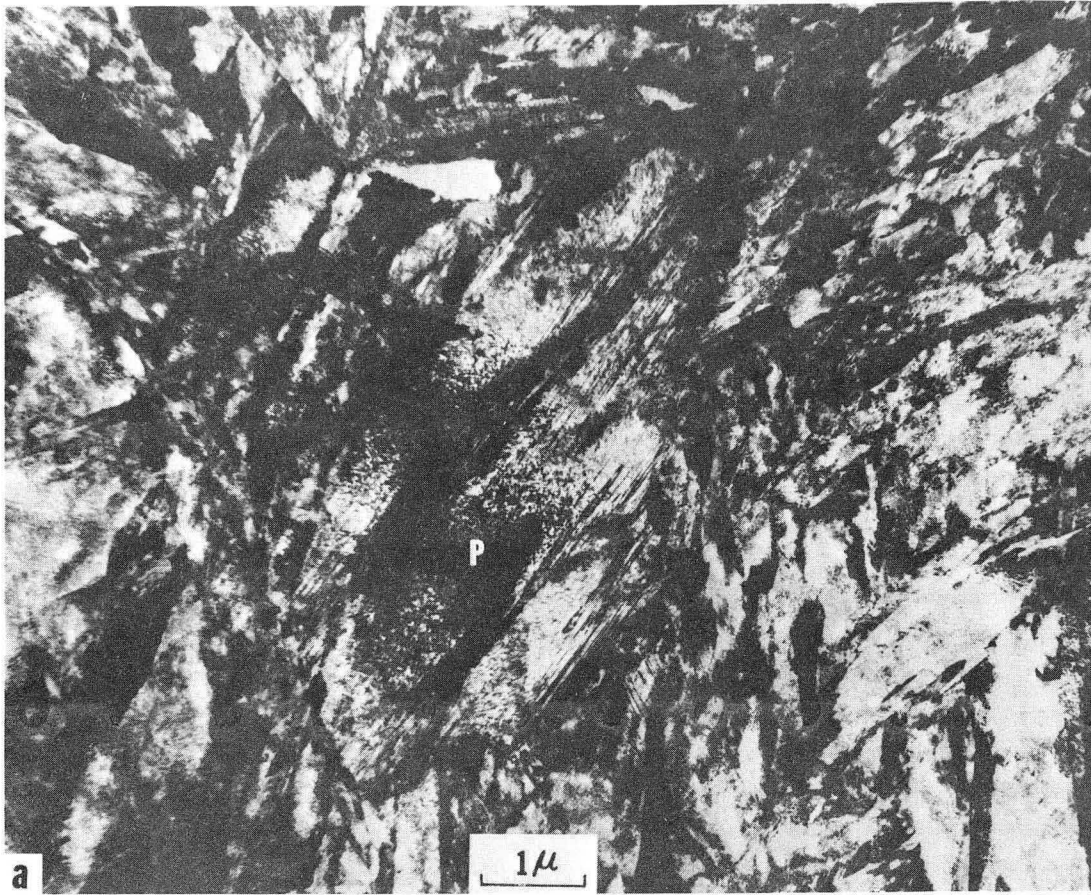
XBB 738-5018

Fig. 20(a)

XBB 738-5028

Fig. 20(b)

Fig. 21

XBL 745-6243

I-T DIAGRAM FOR 4340 STEEL

(As reported by U.S. Steel Corporation)

C-0.42 Mn-0.78 Ni-1.79 Cr-0.80 Mo-0.33

AUSTENITIZED AT 845°C
ASTM GRAIN SIZE: 7-8

XBL 745-6289

Fig. 22(a)

Fig. 22(b)

XBL7311-6666